N69-21392
NASA CR-72516

NASA CR 72516
PWA-3597

CASE FILE
COPY

SEMIANNUAL REPORT NO. 7

DEVELOPMENT OF COMPRESSOR END SEALS STATOR INTERSTAGE SEALS, AND STATOR PIVOT SEALS IN ADVANCED AIR BREATHING PROPULSION SYSTEMS

by

R.M. Hawkins and A.H. McKibbin

Prepared for
National Aeronautics and Space Administration

NASA LEWIS RESEARCH CENTER
CONTRACT NAS3-7605

Pratt & Whitney Aircraft DIVISION OF UNITED AIRCRAFT CORPORATION

EAST HARTFORD, CONNECTICUT

NASA CR 72516
PWA-3597

SEMI-ANNUAL REPORT NO. 7

DEVELOPMENT OF COMPRESSOR END SEALS STATOR INTERSTAGE SEALS, AND STATOR PIVOT SEALS IN ADVANCED AIR-BREATHING PROPULSION SYSTEMS

Prepared for

NATIONAL AERONAUTICS AND SPACE ADMINISTRATION

20 January 1969

CONTRACT NAS3-7605

Technical Management
NASA Lewis Research Center
Cleveland, Ohio

Project Manager
L. P. Ludwig
Fluid Systems Components Division

Written by: R. M. Hawkins
R. M. Hawkins
Project Manager

A. H. McKibbin
A. H. McKibbin
Assistant Project Engineer-Analytical

Approved by: R. P. Shevchenko
R. P. Shevchenko
Senior Project Engineer

Pratt & Whitney Aircraft DIVISION OF UNITED AIRCRAFT CORPORATION

EAST HARTFORD, CONNECTICUT

PREFACE

This report describes the progress of the work conducted between 30 June 1968 and 31 December 1968 by the Pratt & Whitney Aircraft Division of United Aircraft Corporation, East Hartford, Connecticut on Contract NAS3-7605, Development of Compressor End Seals, Stator Interstage Seals, and Stator Pivot Seals in Advanced Air-Breathing Propulsion Systems, for the Lewis Research Center of the National Aeronautics and Space Administration.

Roger M. Hawkins is Project Manager for Pratt & Whitney Aircraft for this program.

The following National Aeronautics and Space Administration personnel have been assigned to the project:

Contracting Officer	J. H. DeFord
Contract Administrator	L. Schopen
Project Manager	L. P. Ludwig

ABSTRACT

The compressor seal test rig was assembled and tested; modifications were made to correct rig discrepancies. Static testing of floating-shoe compressor seals revealed excessive leakage because of tilting of the shoes; modifications were initiated. Vane pivot seals were evaluated at simulated engine conditions and the bellows type exhibited low leakage rates.

SUMMARY

This report describes the work accomplished during the seventh six-month period of an analytical, design, and experimental program directed at developing compressor end seals, stator interstage seals, and stator pivot seals for advanced air-breathing propulsion systems.

Work under Tasks I and III was completed during the first two and one-half years of this contract, and is discussed in the first five semiannual reports. For Task I, this work consisted of feasibility analyses of the one-side and two-side floated shoe seals, the OC diaphragm seal, the semirigid seal, and the flexure-mounted shoe seal. For Task III, the single-bellows vane pivot seal and the spherical-seat vane pivot seal were analyzed. No work on Tasks I and III was carried out during this reporting period, but very brief summaries of the two tasks are included in this report for general background information.

Work under Task II progressed after delivery of the one-side floated-shoe end seal to Pratt & Whitney Aircraft in July 1968. Proximity probes were calibrated and the seal was installed in the test rig. Static tests showed excessive leakage rates, and subsequent investigation indicated that the floated-shoe segments were tilted in respect to the seal plate. A segmented thrust ring was fabricated so that the mating rings could align with greater precision, and vent and bleed holes were added or enlarged. At the end of the reporting period, the modifications were installed in the static bench test fixture for a second room-temperature calibration.

The one-side floated-shoe interstage seal was delivered in October, and static testing showed excessive leakage. This seal will be reworked in the same manner as the end seal and will be re-tested.

Fabrication of the OC diaphragm end seal continued, as did checking of the test rig and the test stand.

Work under Task IV (vane pivot seals) included testing of two single-bellows units and two spherical seat seals at simulated engine conditions; the single-bellows type exhibited low leakage rates.

TABLE OF CONTENTS

LIST OF ILLUSTRATIONS

LIST OF ILLUSTRATIONS (Cont'd)

LIST OF TABLES

INTRODUCTION

Modern high-performance multistage axial-flow compressors built with state-of-the-art features incorporate several air leakage paths which are detrimental to compressor performance. Elimination or significant reduction of these leaks would result in a compressor of higher efficiency and possibly smaller size. Some typical areas of leakage paths with estimates of percent air loss and potential effect on compressor performance are:

	Air Loss	Effect on Compressor Efficiency
End Seal	0.6%	1.0%
Interstage Stator Seals (10 stages)	0.9%	1.0%
Vane Pivot Seals (variable stator)	0.2% per stage	0.2% per stage

Increases in compressor efficiency are traditionally sought by means of compressor geometry redesign. A few extra points in efficiency often mean the difference between a successful or an unsuccessful design. These increases as a result of geometry changes are always very expensive and not always successful. On the other hand, the efficiency losses resulting from air leaks are strikingly large. The gains in efficiency, however, must be balanced against any detrimental effect that improved sealing may have on the engine, such as lower reliability or increased weight.

This program will provide for a research, analytical, and test program having as its goal the development of compressor end seals, stator interstage seals, and vane pivot seals which exhibit lower air leakage rates than those currently in use. Because seal deformation will probably be a major problem area, the components will be of such size, materials, and designs as to be considered to be flight weight and applicable to compressors for advanced engines.

I. TASK I - CONCEPT FEASIBILITY ANALYSIS PROGRAMS FOR COMPRESSOR END SEALS AND FOR COMPRESSOR STATOR INTERSTAGE SEALS

A feasibility analysis was conducted on compressor end seals and stator interstage seal concepts for advanced air-breathing propulsion systems. The first phase of this program consisted of a preliminary analysis and screening of various seal concepts prior to the selection of concepts for the detailed feasibility analysis. The analytical effort included all calculations, analyses, and drawings necessary to establish the feasibility of the selected concepts, and a comparison of the concepts to current practice. This analytical program was subcontracted to Mechanical Technology Incorporated (MTI) of Latham, New York, and was monitored by Pratt & Whitney Aircraft as required under the terms of the NASA contract. The results of the feasibility analysis are reported in Semiannual Reports 1, 2, 4, and 5.

As a result of the concept screening studies, the one-side floated-shoe compressor end seal and stator interstage seal concepts were selected for final feasibility studies. Pratt & Whitney Aircraft submitted the final feasibility designs of these seals to NASA on 19 May 1966 requesting approval to start final design under Task II. Approval was granted in a letter from NASA dated 31 May 1966. Final feasibility analysis of these seals are reported in Semiannual Reports 1 and 2.

Contract Amendment Number 2, effective 15 December 1966, was received from NASA for the feasibility analysis of an OC diaphragm thin-strip seal design. As a backup effort, the contractor also performed a feasibility analysis on a semi-rigid one-piece seal concept. The results of these analyses (see Semiannual Reports 4 and 5), indicated that both seals will yield satisfactory performance. Pratt & Whitney Aircraft subsequently selected the OC diaphragm thin-strip seal for the compressor end seal application and the semirigid one-piece seal for the interstage application.

The feasibility design concepts of the OC diaphragm end seal and the semirigid interstage seal were submitted to NASA on 3 October 1967, and the contractor requested approval to start final flight-weight design under Task II. Approval was granted in a letter from NASA dated 6 November 1967.

II. TASK II - COMPRESSOR END SEAL AND STATOR INTERSTAGE SEAL EXPERIMENTAL EVALUATION

This phase of the program provides for final design and fabrication of compressor end seals and stator interstage seals, design and fabrication of a test rig, and experimental evaluation of the compressor seals.

The final design of the four compressor seal concepts selected for experimental evaluation includes all calculations, material determinations, analyses, and drawings necessary for seal optimization, procurement, and experimental evaluation. A test rig has been designed and fabricated to evaluate the selected compressor end seals and stator interstage seals under simulated compressor operating conditions. The test apparatus simulates the last stages of a full-scale compressor, including supporting members and bearing system in order to faithfully duplicate structural flexibility and thermal gradients.

The compressor end seals and stator interstage seals will be calibrated in incremental steps at room-temperature static conditions, room-temperature dynamic conditions, and subsequently over the full speed, pressure, and temperature operating ranges. The seals will then be subjected to endurance testing and finally will undergo a take-off and cruise cyclic test.

Final design layouts and detailed drawings have been completed for the one-side floated-shoe end and interstage seals, the OC diaphragm end seal, the semirigid interstage seal, and for the full-scale test rig in which the seals will be evaluated. The one-side floated-shoe end seal, the one-side floated-shoe interstage seal, and the full-scale test rig have been procured.

A. ONE-SIDE FLOATED-SHOE END SEAL

The one-side floated-shoe end seal is a face seal consisting of a ring of 24 seal shoe segments acting against a rotating surface (the seal runner) attached to the compressor rotor. Figure 1 is a schematic drawing of the seal. The surface of the seal runner is flat. The primary seal interface is between the stationary ring of shoes and the runner surface, and the leakage flows radially inward through the seal. Secondary seals are provided between the shoes and the carrier ring at the secondary seal pads and the one-piece thrust ring. Another secondary seal is provided between the seal carrier ring and the seal mounting ring at the location of the secondary seal piston ring.

Fabrication of the one-side floated-shoe end seal was completed and the seal was delivered to Pratt & Whitney Aircraft early in July 1968. The assembled seal unit is shown in Figures 2 and 3. The proximity probes and thermocouples were installed at Pratt & Whitney Aircraft, and subsequent calibration revealed that the proximity probes were shorted out. The shorts were burned out by applying approximately 25 volts to the probe terminals and the probes were calibrated to the saturation point. The linear range of the probes was 2 to 3 times the required range, and excellent repeatibility was demonstrated.

After the calibration of the probes, the seal was installed in the test rig and a room-temperature static test was performed. The static test revealed excessive air leakage rates. As shown in Figure 4, the measured air leakage rate was approximately 30 times the calculated rate for any given seal pressure differential. Investigation revealed that the floated-seal shoe segments were tilting with respect to the seal runner.

A static test fixture, shown schematically in Figure 5, was fabricated to allow the contractor to perform several checks on the test seal which could not be performed in the test rig. The static test fixture was designed to allow visual examination of the bore of the seal (including the seal shoe segments) and to allow the measurement of pressures and pressure drops in various regions of the seal. An adapter ring was also designed to allow leakage past the secondary seal piston ring to be measured separately from all other leakage paths. The fixture was also supplied with internal illumination to allow visual checks to ensure that there were no gross leakage paths past the primary or secondary seals.

For the first test of the one-side floated-shoe end seal in the static test fixture, ambient air calibration runs were made to determine whether the fixture would duplicate the rig conditions. The results, which are compared with rig results in Figure 6, show that the fixture gives results comparable with those from the full-scale test rig. Figure 7 shows the corresponding apparent air-film thickness as measured by the proximity probe.

As pressure was gradually increased, the seal carrier ring suddenly moved axially about one-eight inch away from the seal runner. A corresponding jump occurred in the reading of the proximity probes. This jump is illustrated in Figure 7. When pressure was reduced, the carrier returned to its initial position. The jump away from the seal runner has been explained as the result of excessive leakage, causing a pressure imbalance resulting in a net force pushing the seal carrier ring back.

A 2-mil feeler gauge was used to check the separation between the shoe seal segments and the seal runner. The gauge could be inserted at the inner edge of the shoes and pushed halfway across the shoe toward the outer edge, indicating that the shoes were tilted. An attempt was made to observe the tilt by shining a light on the outer edge of the shoe and observing the slit light pattern at the inner edge; no definitive conclusions could be drawn from the light patterns because of slight surface irregularities and edge diffraction effects.

Tactile examination of the leakage flow indicated excessive flow through the shoe low-pressure vent holes, and a lesser flow through the primary seal interface. The secondary seal piston ring with the rectangular cross-section had no discernible leakage.

The seal was removed from the fixture and disassembled. Clearly outlined on the fixture were dust imprints of the shoe seal segments, with a heavy concentration about the outer edge, especially near the shoe center. These dust imprints confirmed that the shoes were tilting in such a manner that a gap was created between the inner edge of the shoes and the seal runner.

To alleviate the tilting, a segmented thrust ring has been fabricated to replace the one-piece ring formerly in use. The new segments will allow the beveled thrust rings to align themselves with greater precision. This change also allows the spring radial load component against the shoe to be directed more positively toward the two secondary seal pads. In addition, eight low-pressure vent holes have been added to the existing three low-pressure vent holes in each of the 24 shoes, 96 high-pressure bleed holes have been added to the seal carrier ring, and the existing 48 high-pressure bleed holes have been enlarged. At the end of the reporting period, the seal had been reinstalled in the static test fixture and was ready for a second room-temperature calibration.

B. ONE-SIDE FLOATED-SHOE INTERSTAGE SEAL

The one-side floated-shoe interstage seal is very similar to the one-side floated-shoe end seal shown in Figure 1. The only differences between the seals are those caused by the slightly different mechanical requirements for sealing in the end and interstage positions.

Most of the work on the one-side floated-shoe interstage seal during this reporting period was concerned with fabrication. Some difficulty was encountered with the hardcoat on the floating-shoe seal segments. The shoes were coated with aluminum oxide (LA-2), which chipped during the final machining operation. Recoating and remachining solved the problem and the parts were brought to the correct dimensions. Once the hardcoating problem had been solved, the shoes were instrumented with proximity probes and thermocouples and assembled in the seal.

Fabrication and assembly of the seal were completed in October, and the seal was shipped to Pratt & Whitney Aircraft. The assembled seal is shown in Figures 8 and 9. When the seal was received, inspection checks were performed on some of the more accessible critical dimensions, such as the depths of the Rayleigh pads and the end gaps between the floating-shoe seal segments.

The preliminary checkout of the one-side floated-shoe interstage seal was performed in a static test fixture similar to that used for the end seal. The fixture is shown schematically in Figure 10. The preliminary static checkout of the seal showed results similar to those from the static check of the end seal: leakage was excessive and there is the same sudden increase in film thickness between seal pressure differentials of 30 and 40 psi. The leakage is shown in Figure 11 and the reading of the proximity probe is shown in Figure 12. At the end of the reporting period, it was decided that the interstage seal would be reworked in the same manner as the end seal. The thrust ring will be segmented, low-pressure vent holes will be added to the shoes, existing high-pressure bleed holes in the seal carrier ring will be enlarged, and additional high-pressure holes will be machined in the seal carrier ring.

C. OC DIAPHRAGM END SEAL AND SEMIRIGID INTERSTAGE SEAL

The OC diaphragm end seal (shown schematically in Figure 13) employs a thin, flexible one-piece strip as the primary seal element, providing a high degree of conformity to runner distortion. The thin strip is supported by three C-shaped semitoroidal diaphragms mounted on a floating seal carrier ring. The seal carrier ring provides for axial travel relative to the main engine structure, and a secondary seal piston ring is used between the carrier and the seal mounting ring. One of the C diaphragms forms a seal between the high-pressure and the low-pressure areas. The other two C diaphragms face each other and form a chamber to which the high-pressure air is admitted. This design, therefore, permits direct balancing of the moments on the thin strip. The OC design does not use the T-section strip required to properly balance moments in the thin-strip designs previously considered. It also permits a decrease in the thickness of the strip relative to other thin-strip designs. Thus, it offers the opportunity of generating a section with increased flexibility and better tracking capability. Furthermore, the moment balance is achieved with methods which are more nearly independent of angular displacements of the strip, making a low residual moment imbalance easier to achieve.

The semirigid interstage seal (shown schematically in Figure 14) operates on the same basic principle as the OC diaphragm end seal: leakage is controlled by controlling clearance. Primary sealing is accomplished at the seal face, which consists of a single land. This land has a spiral-groove inherently compensated orifice profile, and acts as a bearing and seal combination. The angular stiffness of a single land bearing is very low. As a result, the seal ring must be rigid enough to absorb residual bending moments without appreciable deformation of the seal face. To accomplish this, substantial seal-ring axial length is required. Moreover, the seal ring must also serve as a housing for the piston ring required for secondary sealing, one of the seals being formed by contact between the side of the piston ring and the seal ring. It should be noted that the combination of seal axial length and piston-ring contact is conducive to the generation of high thermal gradients. Thermal gradients in turn cause the seal surface to deform, and through this deformation they may seriously affect seal performance. In order to minimize the extent of thermal gradients and seal deformations, the following steps have been taken:

- Duranickel 301 was selected as the seal material to provide high thermal conductivity in combination with an adequate coefficient of thermal expansion. Commercially pure nickel was considered for the seal, but it appeared that this material would lack structural strength and would have undesirable creep properties. Molybdenum alloy TZM would provide excellent thermal conductivity and a substantially lower coefficient of expansion, but would be prhibitively expensive.

- The secondary seal piston ring was insulated through the inclusion of a thermal barrier in the form of a radial annular slot.

- The cross section of the primary seal element was designed to minimize thermal distortion through the use of a nearly constant temperature projection on the seal's outer edge close to the seal face.

- The seal's tracking performance characteristics indicate tolerance to some degree of distortion. Thermal distortion produces a convergent flow path, as described in Semiannual Reports 4 and 5 (PWA-3147 and 3302). The seal was designed so that if slight convergent distortion occurs, the net result is an increase in flim thickness , reduction in heat generation at the seal face, and an increase in leakage flow. The increased airflow carries more heat away from the seal face, leaving less heat to be dissipated by the seal and therefore, lower thermal gradients, and a modulated thermal distortion.

The seal ring is preloaded with 24 helical coil springs to ensure contact at start and to permit the development of separating air films at speeds under 30 ft/sec. Both the seal face and runner are hardcoated with chrome carbide. This combination was selected with regard to compatibility at high temperature and resistance to wear. This material is identical to the hardcoat used for the OC diaphragm seal.

All of the work on the OC diaphragm end seal and the semirigid interstage seal during this reporting period has been concerned with seal fabrication. Purchase orders for both seals were approved by NASA in August, 1968 and orders for the seals were placed with the vendor in the same month. At the end of the reporting period, many small detail parts had been completed and nearly all of the rough machining had been completed. Some finish work and heat treating had also been completed.

D. COMPRESSOR SEAL TEST RIG

Early in the reporting period, the test rig was mounted on the rig transporter and installed in the test stand in preparation for the initial checkout. The rig is shown mounted on the transporter in Figure 15 and installed in the test stand in Figure 16. The initial checkout was conducted for about five hours at speeds ranging up to 7500 rpm. Once a starting procedure had been worked out, the rig presented no running problems, and vibration levels were very low. When the initial checkout had been completed, the rig was disassembled for inspection, which revealed several discrepancies.

When the splined jumper shaft was removed from the rig, it was found that some of the spline teeth had worn. The shaft was reoperated to dress the teeth and to provide more clearance for oil flow through the splines. To reduce wear in the future, the splines were flashed with AMS 2406 chrome to a thickness of 0.0004 to 0.0005 inch. When the rig was further disassembled, it was discovered that the main roller bearing had failed. Some of the rollers and several areas on the outer race were severely scored, apparently, because of the high preload on the bearing. To alleviate this condition, most of the preload was removed, and the bore of the bearing was increased to the maximum possible diameter. During the initial checkout, it had been found that there was an interference in the linkages which controlled the axial movement of the cases, so the cases and the links were reoperated to remove the interference. To eliminate a slight sag of the rig case on the supporting rollers, a stiffener ring was made and pinned in place on the thrust-bearing end of the case. This ring surrounds the support pads and prevents them from deflecting. The seal centerline will therefore remain parallel and coincident with the disk centerline within dimensional limitations.

When the rework had been completed, the test rig was reassembled with the one-side floated-shoe end seal in place. All thermocouples for the rig and seal were checked out after the rig had been reassembled. Some were found to be inoperative, but this condition was not considered to be a problem because of built-in redundancy. The final step in the rebuild of the rig was the machining of additional ports in the seal leakage compartment of the rig case to ensure the attainment of low back pressure on the test seals. Since that time, the rig has been installed on the test stand and used in the preliminary checkout of the one-side floated-shoe end seal. The operation of the rig was normal, and no further discrepancies were noted when the rig was disassembled to remove the test seal.

E. TEST STAND

The principal work performed on the test stand during this reporting period was the correction of a combustion instability which was discovered at the end of the previous reporting period. The instability was traced to the burner can, which was reworked to a new configuration. The reworked can was tested in a burner stand, and showed satisfactory performance over a range of flows equal to those required for the Task II tests. The burner was then reinstalled in the test stand. The heater was successfully lit off six times, and operation was satisfactory over a range of air flows. However, continued calibration of the burner system revealed an unstable condition when using the low flow secondary portion of the burner fuel nozzle. It was decided that a fuel nozzle having sufficient primary flow to eliminate the need for secondary fuel flow would be used. Several nozzles were tried and an early JT9D nozzle was selected for use in the burner assembly. This nozzle has excellent characteristics at high fuel and air flows on primary supply alone. However, it is slightly unstable at the lowest flows. This will not be a problem, however, as two different bleed systems are available. An adequate burner flow for stable operation without compromising seal or rig performance will, therefore, be used.

In addition to the work on the burner, some minor revisions to the stand plumbing were made to facilitate pressure control in the rig and to increase the accuracy of some flow measurements. To guard the rig against excessive pressure, high-temperature pressure relief valves were installed in the air lines.

When these modifications had been completed, the stand was used for the first static test of the one-side floated-shoe end seal. The operation of the stand was normal in every respect, and no new problems were encountered.

III. TASK III - COMPRESSOR STATOR PIVOT BUSHINGS AND SEAL CONCEPT FEASIBILITY ANALYSIS

A feasibility analysis program was conducted on stator vane pivot bushing and seal concepts for application in compressors for advanced air-breathing propulsion systems. The first phase of this program consisted of a preliminary analysis and a screening of various seal concepts prior to the selection of concepts for the detailed feasibility analysis. The analytical effort included a comparison of the selected concepts to current practice and all calculations, analyses, and drawings necessary to establish the feasibility of these selected concepts. This analytical program was subcontracted to Mechanical Technology Incorporated (MTI) of Latham, New York, and was monitored by Pratt & Whitney Aircraft as required under the terms of the NASA contract.

Work under Task III has been completed. Pratt & Whitney Aircraft submitted the latest feasibility designs of the single-bellows and spherical-seat vane pivot seals to NASA on 19 May 1966, requesting approval to start final design of these seals under Task IV. An effort was made to simplify the seal designs within practical limits without making major changes in the basic seal concepts shown on the MTI drawings. Approval was granted in a letter from NASA dated 31 May 1966.

IV. TASK IV - PIVOT BUSHING AND SEAL EXPERIMENTAL EVALUATION

A. INTRODUCTION

This phase of the program provides for final design and procurement of bushings and seals, design and fabrication of a test rig, and experimental evaluation of bushing and seal assemblies. The final design of the two selected concepts for experimental evaluation includes all calculations, material determinations, analyses, and drawings necessary to optimize pivot bushings and seals.

The contract requirement for experimental evaluation of four variable-stator pivot seals has been completed. Two single-bellows and two spherical seals were tested under conditions which simulated the final compressor stage of an advanced engine. Each seal was calibrated in increments over the full pressure and temperature range, with a maximum pressure drop across the seals of 135 psig and a maximum air temperature of 1200°F. One seal of each design was tested for forty hours. For the bellows seals, the air leakage rates were slightly less than the calculated values. For the spherical seals, the leakage rates were considerably higher.

B. SINGLE BELLOWS SEAL

The first single-bellows test unit (Figure 17) was calibrated according to the schedule shown in Table I. Leakages are in SCFM, torques are in inch-pounds.

TABLE I
CALIBRATION SCHEDULE

	Pressure													
	20		40		60		80		100		130		135	
AIR TEMP. °F	Leakage (SCFM)	Torque (IN-LBS)	Leakage (SCFM)	Torque (IN-LBS)	Leakage (SCFM)	Torque (IN-LBS)	Leakage (SCFM)	Torque (IN-LBS)	Leakage (SCFM)	Torque (IN-LBS)	Leakage (SCFM)	Torque (IN-LBS)	Leakage (SCFM)	Torque (IN-LBS)
Room Temp.	*	6	*	6	*	6	*	6	*	6	*	4	*	3
200	*	3	*	3	*	3	*	3	*	2	*	2	*	2
400			*	2	*	2	*	2	*	2	*	1.6	*	1.6
680			*	3.2	*	2	*	2	*	2	*	2	*	2.4
800			*	4.8	*	4.8	*	6.4	*	8	*	8		
1000					*	7.2	*	7.2	0.100	7.2				
1200					0.031	6.4	0.052	6.4						
ROOM TEMP	*	20+	0.00023	20+	0.0014	20+	0.007	20+	0.011	20+	0.014	18.4	0.0177	17.6

* Less than Capability of Instrumentation

Vane Bending Load - 30 in-lbs Static
- ± 4.5 in-lbs superimposed at 1725 cps.

Vane Actuation - ± 6° Oscillation at 9.6 cpm

The simulated dynamic and superimposed vibratory bend moments remained the same throughout the calibration. This seal was subsequently endurance tested for 20 hours at simulated sea-level take-off conditions and for 20 additional hours at simulated cruise conditions. The results are shown in the curves of Figures 18 and 19. As can be seen, seal leakage compares favorably with the design forecast of 0. 00079 SCFM.

A second single-bellows seal was tested according to the calibration schedule and actuation torque of Table II.

TABLE II

STATOR PIVOT SEAL - SINGLE BELLOWS CALIBRATION
SCHEDULE AND ACTUATION TORQUE

Seal ΔP PSIG	20	40	60	80	100	120	135	VANE BENDING MOMENT
				VANE ACTUATION TORQUE IN-LBS				
Air Temp °F								
Initial R. Temp.	8.3	9	9	11.6	11.3	10.5	11.3	30 in-lbs
200	13.5	12.4	12	9	8.3	7.5	8.6	
400		9.5	8.5	9.5	9.5	8.5	9.5	
680		11.3	10.9	13.1	13.1	13.9	13.5	
800		15	14.5	13	14	13.5		
1000		3.6	3.7	4.2	4.8	5.0		10 in-lbs
1200			4.4	4.8	5.2			
Final R. Temp.	19.5	15	15.5	15.5	16	16	15	30 in-lbs

The schedule shown in Table II may be correlated with the seal leakage curves shown in Figure 20.

Changes were made in the calibration schedule of Table I: test points were added, and the vane bending moment was reduced from 30 inch-pounds to a more realistic 10 inch-pounds at the 1000°F and the 1200°F test points to more realistically simulate cruise conditions. This seal also performed favorably.

C. SPHERICAL SEAT SEAL

The third unit to be tested was a spherical seat seal. It was subjected to the pressures, temperatures, and vane bending moments indicated in Table III.

TABLE III
VARIABLE STATOR PIVOT SEAL - NAS3-7605
CALIBRATION SCHEDULE AND VANE ACTUATION TORQUE - IN-LBS
TEST UNIT #3

	Air Temp	Seal ΔP - Rig Pressure 20 PSIG	40 PSIG	60 PSIG	80 PSIG	100 PSIG	120 PSIG	135 PSIG
	Initial Room Temp	15	15	15	15	15	15.5	16
	200°F	13.5	14	13	13.5	13	14	13.5
	400°F		13	13.5	12.5	12.5	13	13 Take Off
Vane Load 30 In-Lbs ±15% Vib	680°F		11.5	14	14	14	14	15
	800°F		14.5	16.5	17	17	17	
Vane Load 10 In-Lbs ±15% Vib	1000°F		6.3	7.5 Cruise	6	6		
	1200°F		6	4.5	4.5	4.5		
Vane Load 30 In-Lbs ±15% Vib	Final Room Temp	14.5	14.5	14.5	15	16	16	16

Performance of this seal deteriorated as the test progressed. The design forecast for this seal was 0.0004 SCFM at a ΔP of 135 psig. It is apparent from the curves of Figure 21 that the ability to seal deteriorated as the test progressed. Two explanations can be put forth: As the carbon seat began to wear, the debris collected as small accumulations of carbon between the sealing interfaces created an air gap and thus providing a leakage path. Another possible explanation is the failure of the seat to find a positive sealing position with the mating spherical seal when the vane is cocked under the bending moment. This situation was suggested when a second spherical seal unit was calibrated and endurance tested.

Performance of a second seal (Test Unit 4) was also less than expected (Figure 22). Calibration (Table IV) was only slightly better than the first seal. During testing, the misalignment of the seat and the spherical seal became apparent. It can be seen from the endurance leakage data points plotted in Figure 23 that at

TABLE IV
VARIABLE STATOR PIVOT SEAL - NAS3-7605
CALIBRATION SCHEDULE AND VANE ACTUATION TORQUE - IN-LBS
TEST UNIT #4

	Air Temp	Seal ΔP - Rig Pressure 20 PSIG	40 PSIG	60 PSIG	80 PSIG	100 PSIG	120 PSIG	135 PSIG
	Initial Room Temp	12.8	12	11.3	12.5	12.5	13	13
	200°F	13.5	13	13.5	12.5	13	14	14
	400°F		12	12	13	14	15	15
Vane Load 30 In-Lbs ±15% Vib	680°F		13.5	13.5	15.5	18.5	20	Take Off 20
	800°F		18	17.3	17.3	17.3	18	
Vane Load 10 In-Lbs ±15% Vib	1000°F		4	4	4	4		
	1200°F		4.1	Cruise 4.1	4.1	4.8		
Vane Load 30 In-Lbs ±15% Vib	Final Room Temp	18.5	19	20	20	21	23.1	22.8

sea-level take-off conditions, the seal performance was very erratic when the vane bending moment is greatest. At cruise conditions, with a light bending moment, the seal performance was steady with a relatively low leakage. The curve through the SLTO data points of Figure 23 represents a limited computer effort to find an equation to describe the test data. The equation determined was:

$$y = C_1 + C_2 e^{x} + C_3 x$$

where

y = seal leakage, SCFM
x = time, hours
$C_1 = 0.743316 \times 10^{-2}$
$C_2 = 0.412958 \times 10^{-11}$
$C_3 = 0.237885 \times 10^{-3}$

The vane actuation torque (Figure 24) was high in all four test units because there was a high coefficient of friction between the AMS 5663 vane sleeve and the AMS 5387 bushing. In an effort to reduce this friction, a vane sleeve with a hard-coat of tungsten carbide flame spray has been ordered. This new sleeve will be tested with a bushing of AMS 5387. Material combinations for the four variable stator seals tested are given in Table V.

TABLE V

VARIABLE STATOR SEAL MATERIAL COMBINATIONS

Single Bellows

Part	Test Unit	Material
Vane Sleeve	1	AMS 5663 N. Alloy
	2	AMS 5663 N. Alloy
Seal Seat	1	Hardface - Tungsten Carbide
	2	Hardface - Chrome Carbide
Seal	1	Hardface - Tungsten Carbide
	2	Hardface - Chrome Carbide
Housing Bushing	1	AMS 5387 Cobalt Alloy
	2	AMS 5387 Cobalt Alloy

Spherical Seat

Part	Test Unit	Material
Vane Sleeve	3	AMS 5663 N. Alloy
	4	AMS 5663 N. Alloy
Spherical Seal	3	Hardface - Chrome Carbide
	4	Hardface - Tungsten Carbide
Spherical Seat	3	56HT Carbon
	4	AMS 5387 Cobalt Alloy
Housing Bushing	3	AMS 5387 Cobalt Alloy
	4	AMS 5387 Cobalt Alloy

After test, the mating seal surfaces of the single-bellows configuration revealed light rub paths and slight discoloration due to high-temperature effects. At the conclusion of testing, the seal interface surfaces of the spherical-seal design appeared to be highly polished. The 56HT carbon seal seat was worn considerably. Metallic seal parts were slightly discolored after being subjected to temperatures reaching 1200°F.

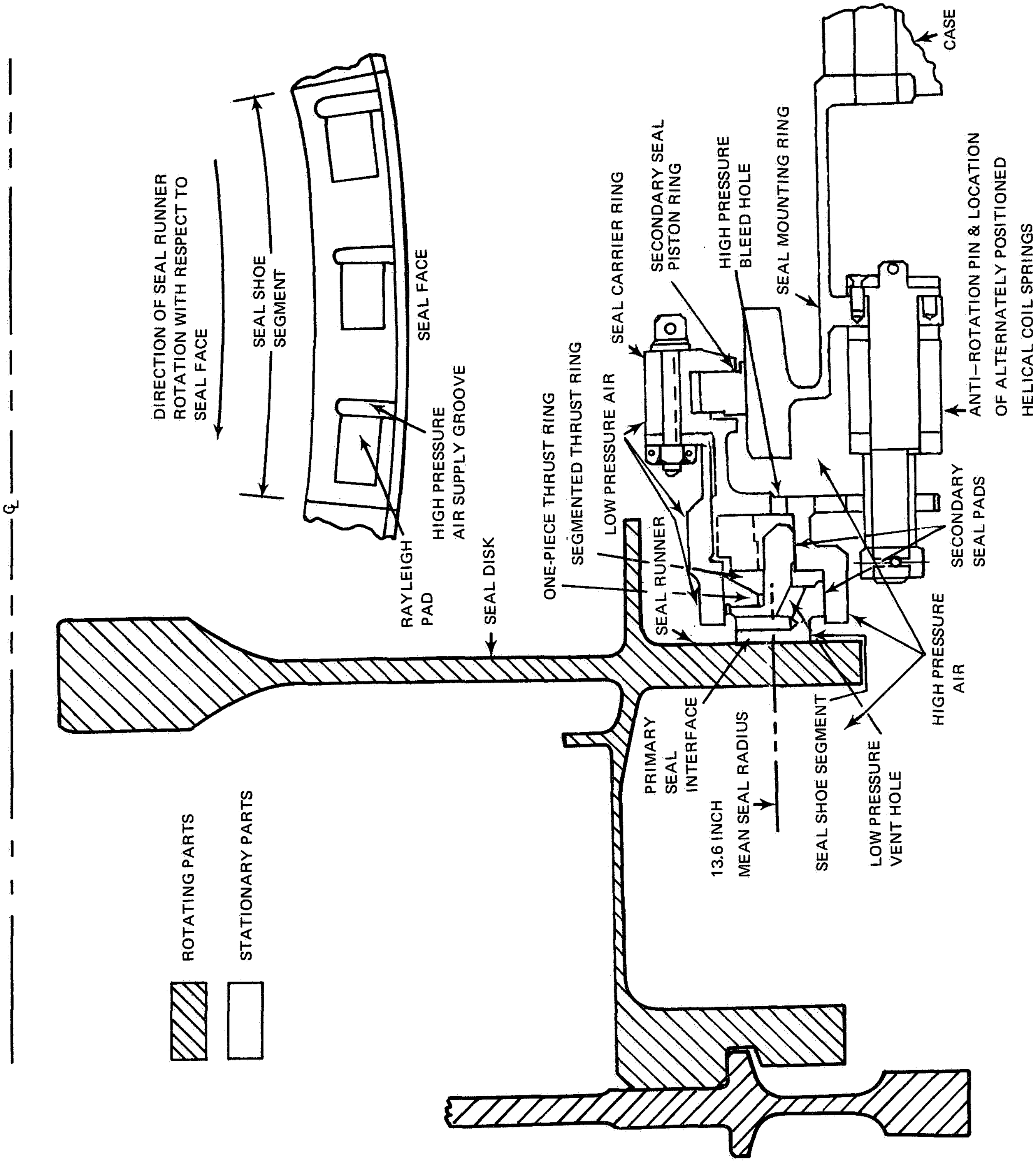

Figure 1 Schematic of the One-Side Floated Shoe End Seal

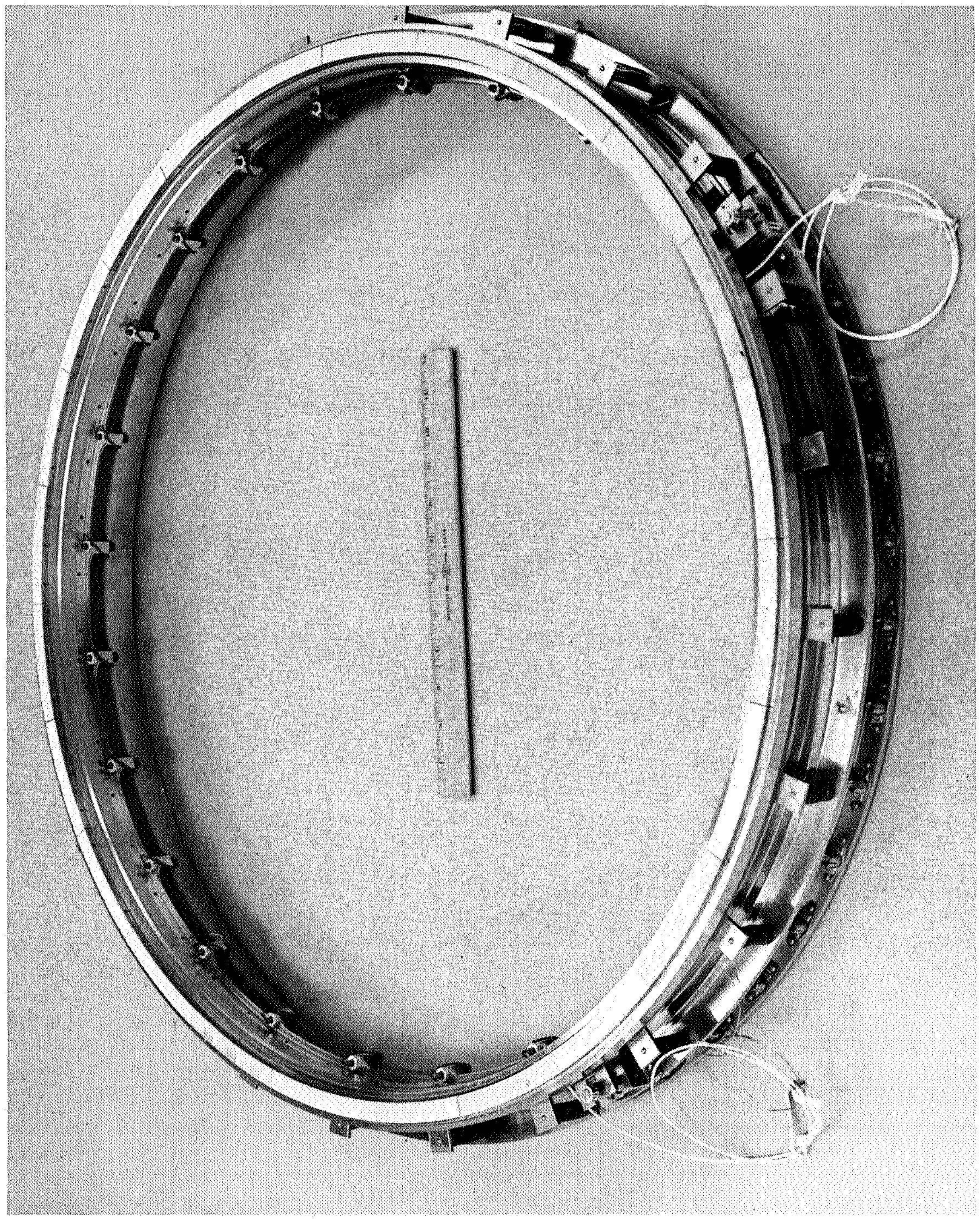

Figure 2 One-Side Floated-Shoe End Seal (CN-14385)

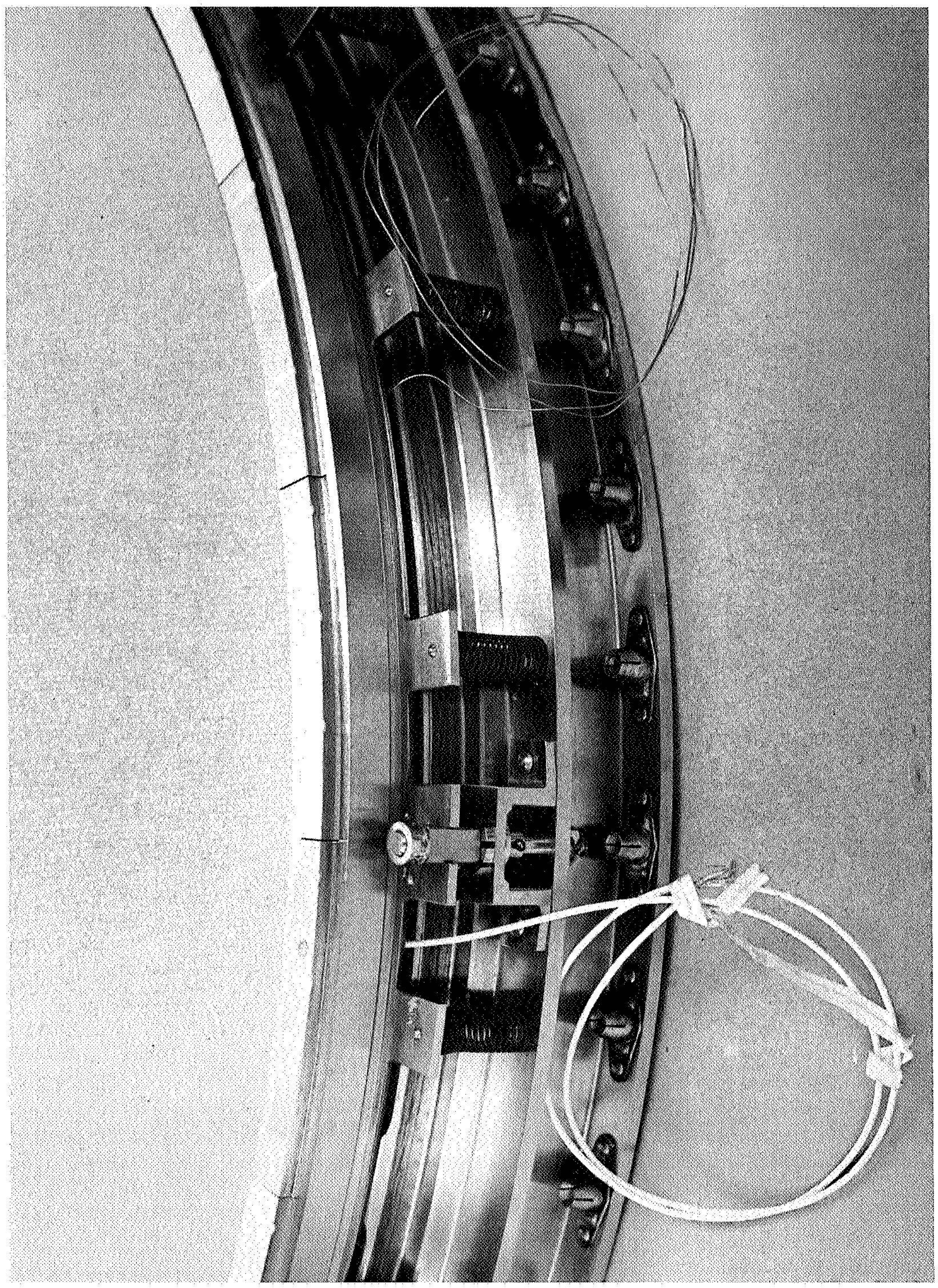

Figure 3 Side View of the One-Side Floated-Shoe End Seal (CN-14386)

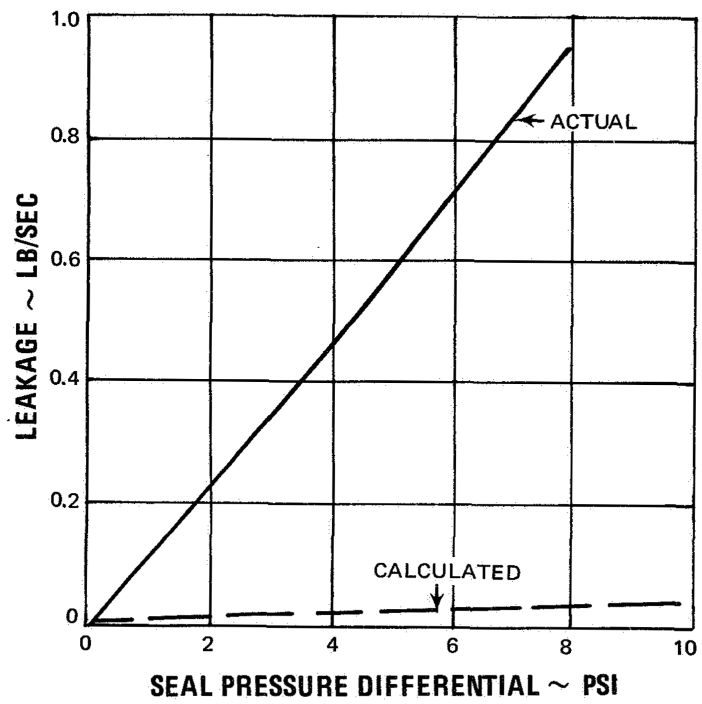

Figure 4 Initial Room Temperature Static Calibration of the One-Side Floated-Shoe End Seal

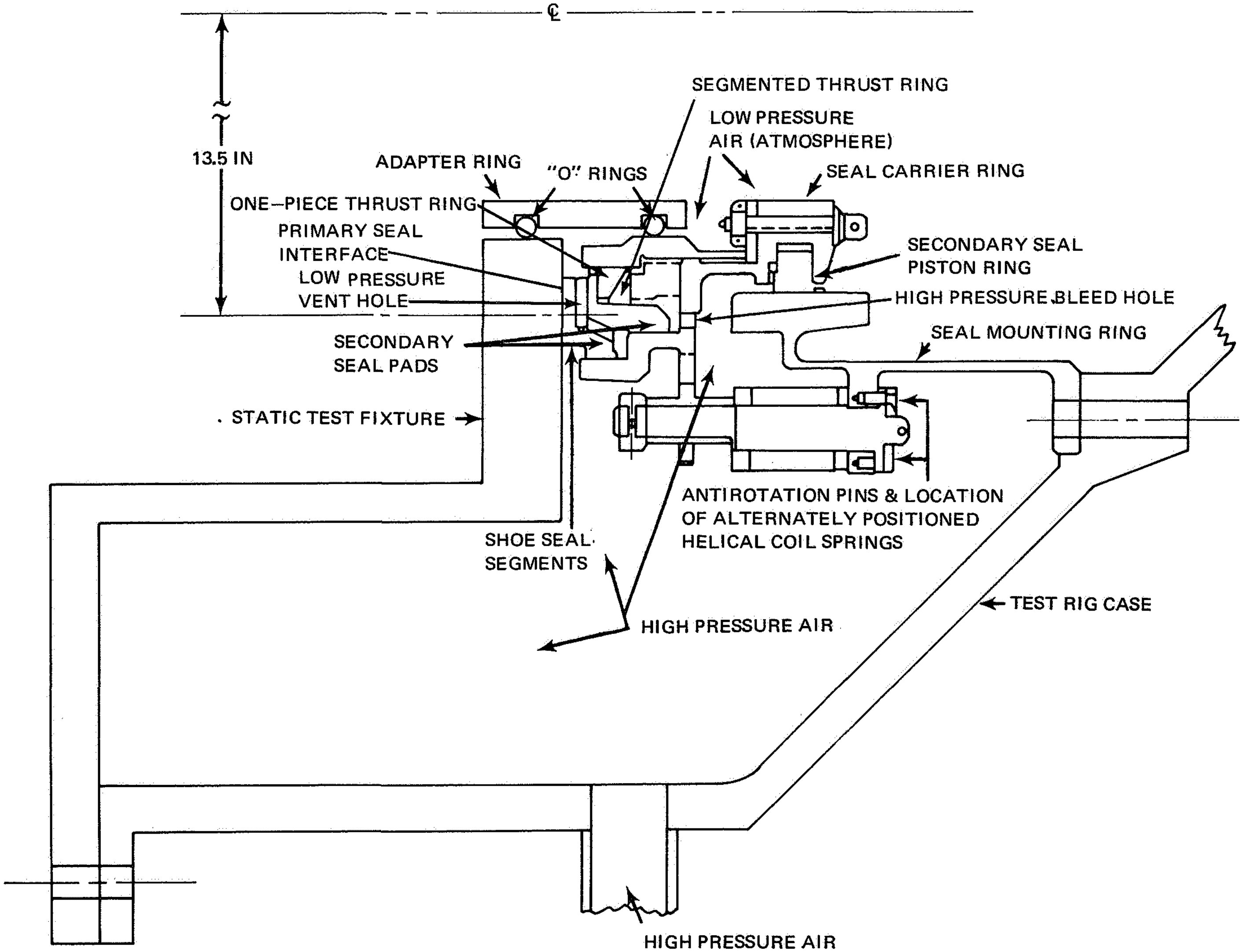

Figure 5 Cross Section of Fixture for Static Test of the One-Side Floated-Shoe End Seal

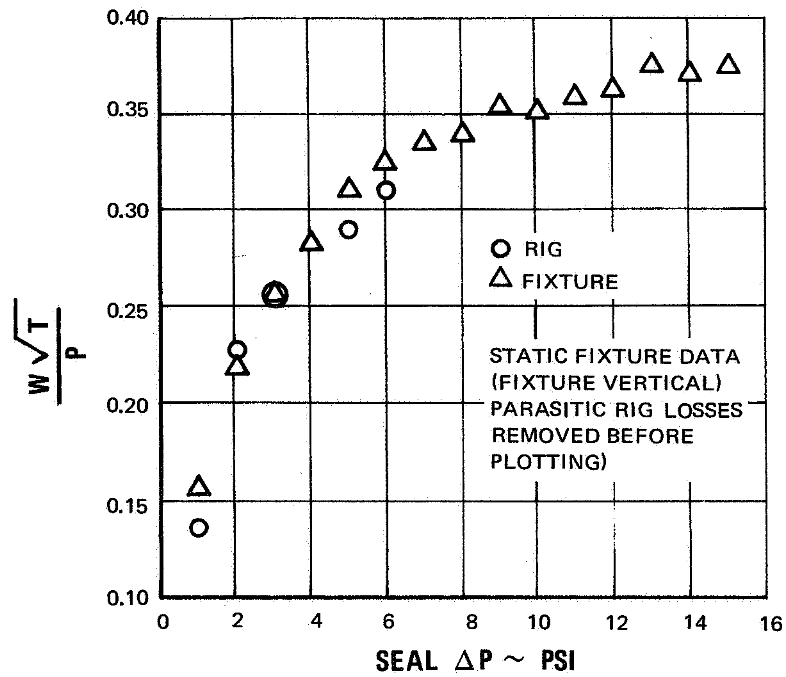

Figure 6 One-Side Floated-Shoe End Seal, Ambient Air Calibration at Static Conditions

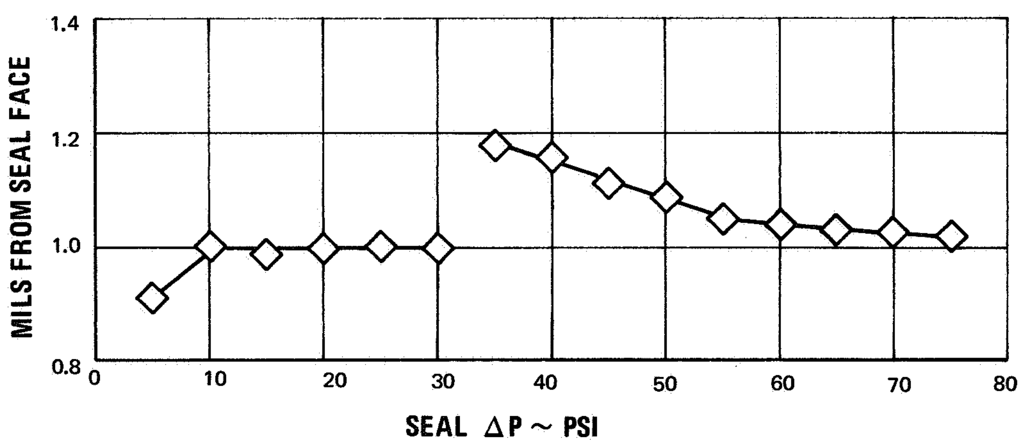

Figure 7 One-Side Floated-Shoe End Seal, Ambient Air Calibration at Static Conditions. Proximity Probe Reading with Static Fixture Held Vertical

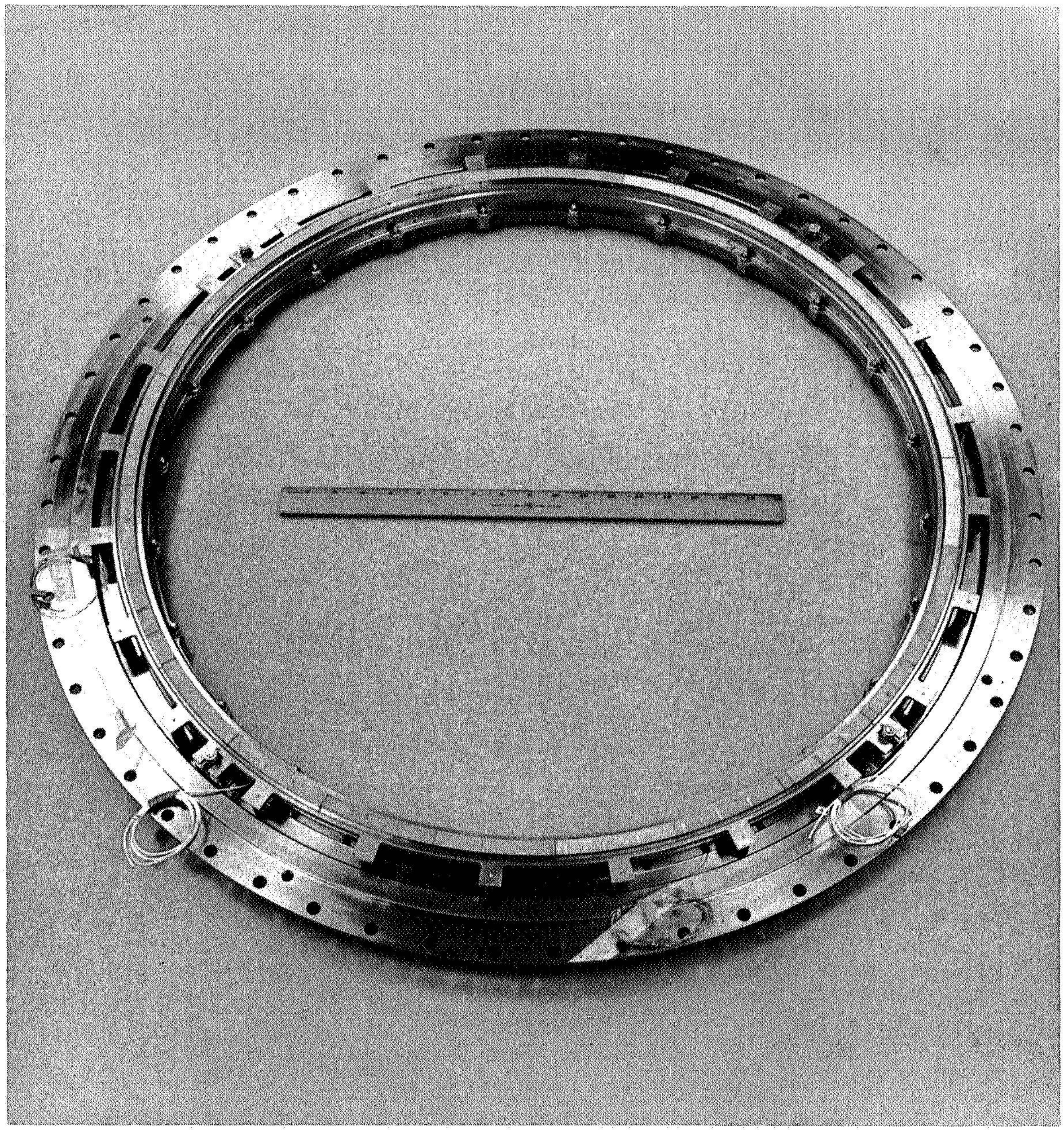

Figure 8 Over-All View of Air Film Riding Sealing Face of Floating Shoes (WCN-48)

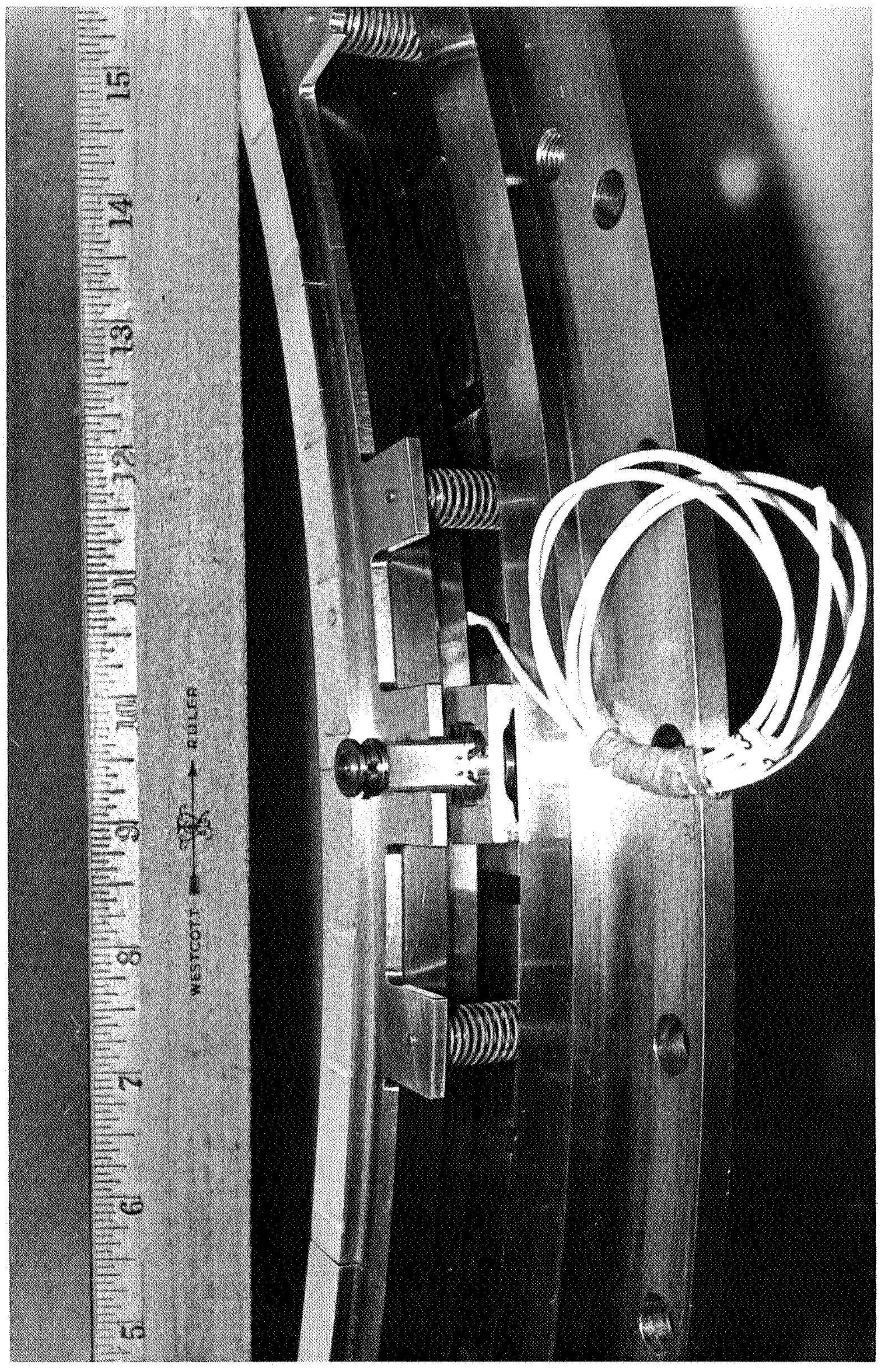

Figure 9 Close-Up View of Front of One-Side Floated-Shoe Seal Showing Proximity Probe and Anti-Torque Pin with Indexing Slots (WCN-50)

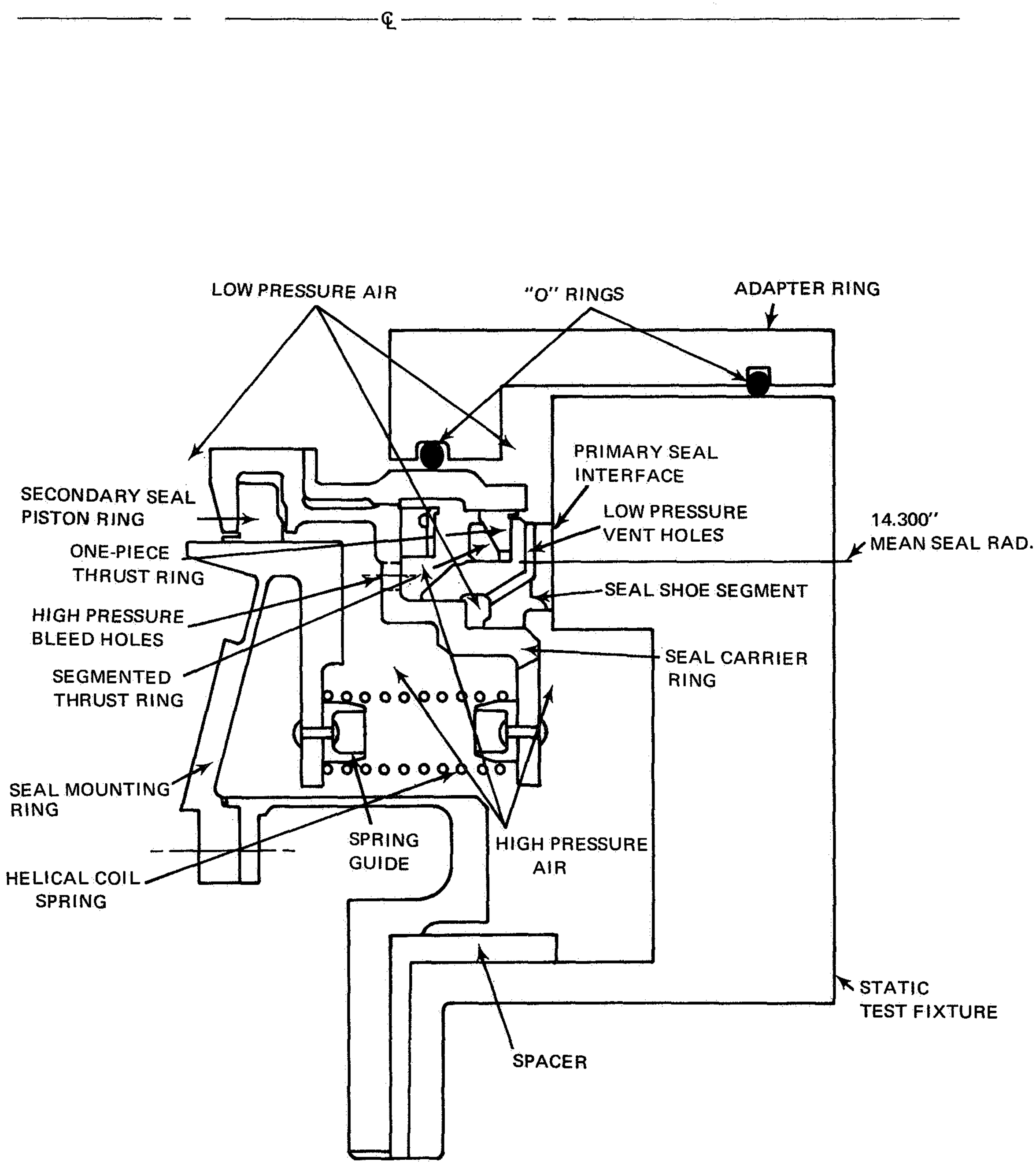

Figure 10 Cross Section of Fixture for Static Test of the One-Side Floated-Shoe Interstage Seal

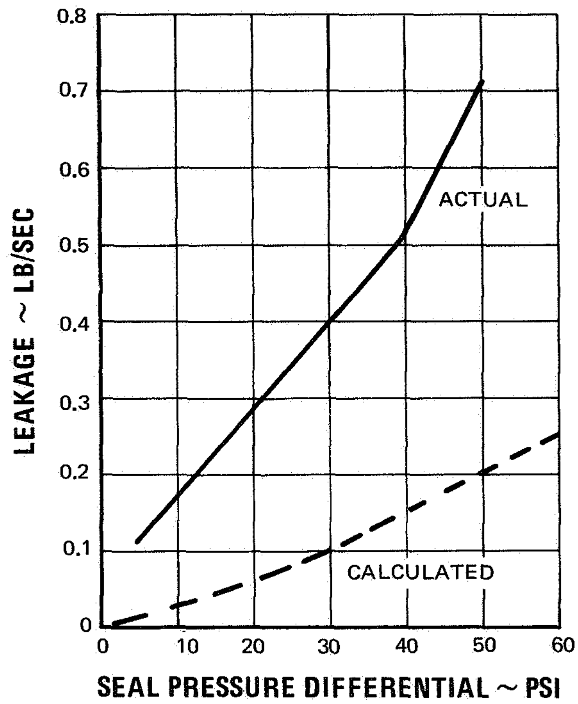

Figure 11 Ambient Air Calibration of the One-Side Floated-Shoe Interstage Seal in Static Fixture

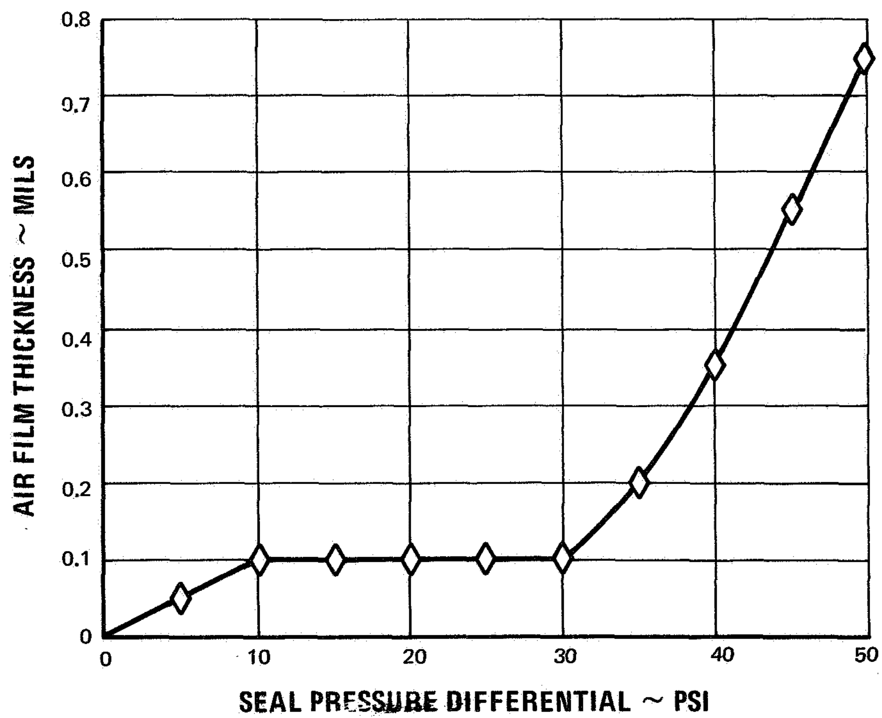

Figure 12 Primary Seal Air Film Thickness. Ambient Air Calibration of One-Side Floated-Shoe Interstage Seal in Static Fixture

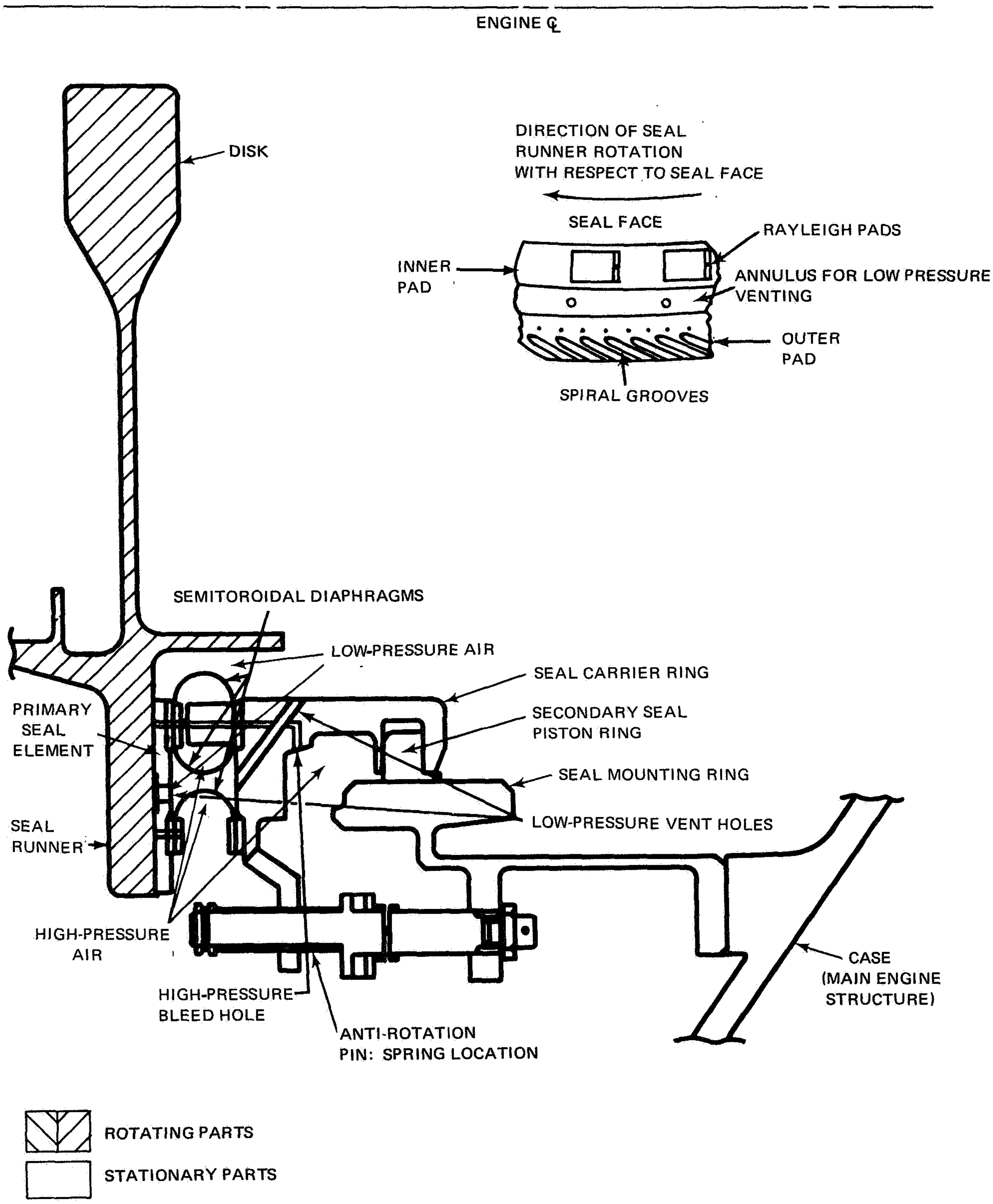

Figure 13 OC Diaphragm End Seal

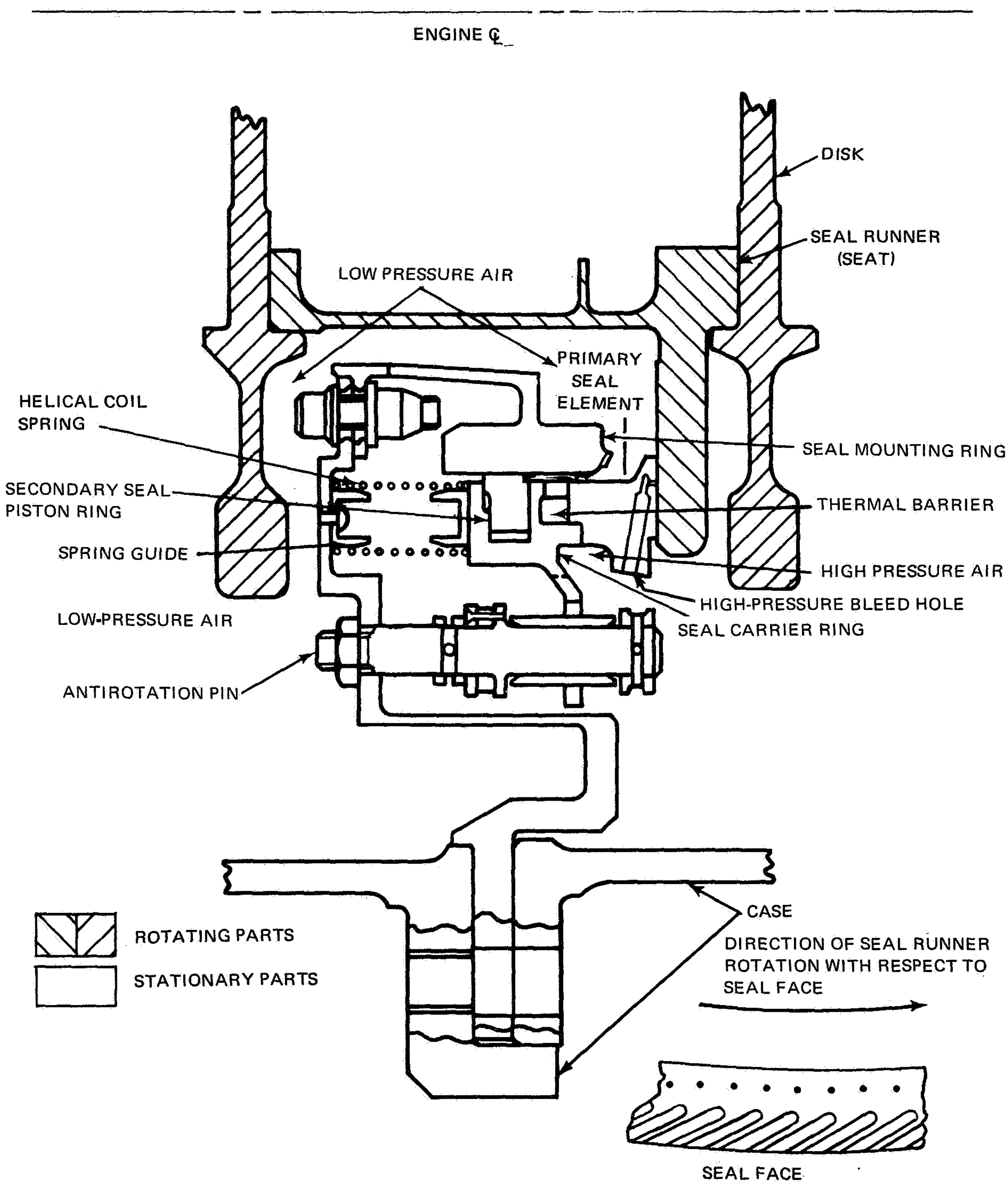

Figure 14 Semirigid Interstage Seal

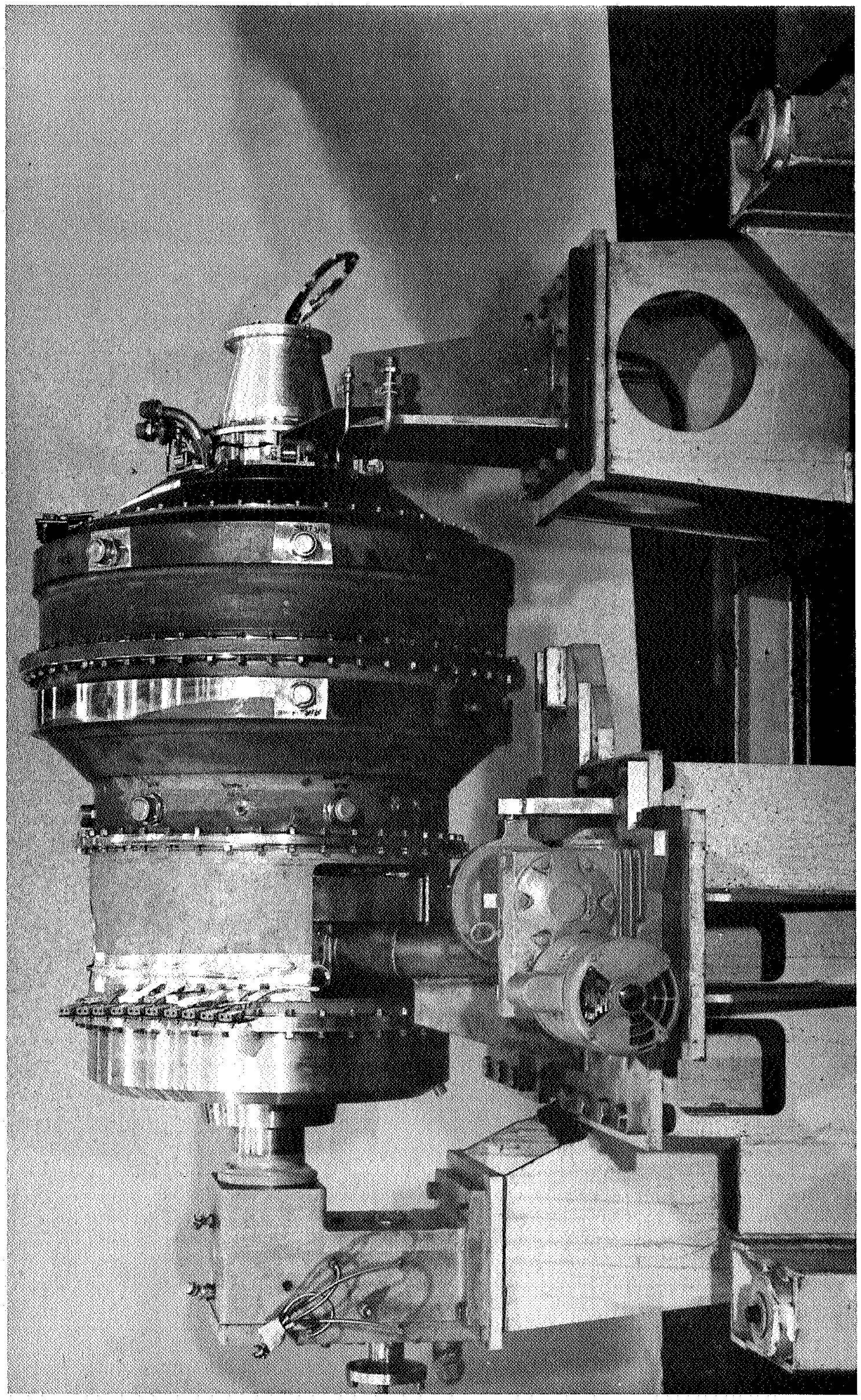

Figure 15 Compressor Seal Test Rig Mounted on Rig Transporter (CN-13744)

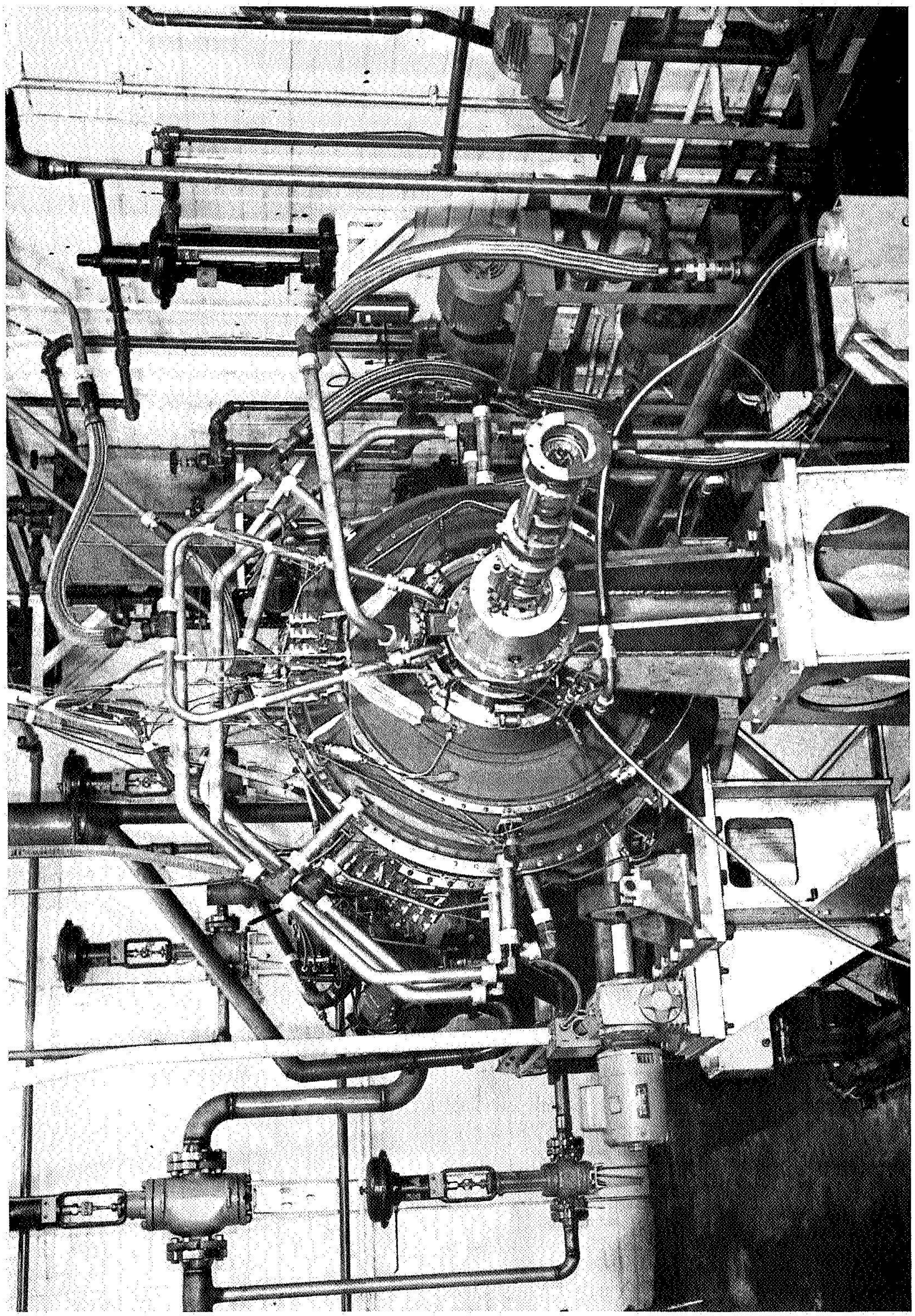

Figure 16 Compressor Seal Test Rig Mounted in Stand (CN-14690)

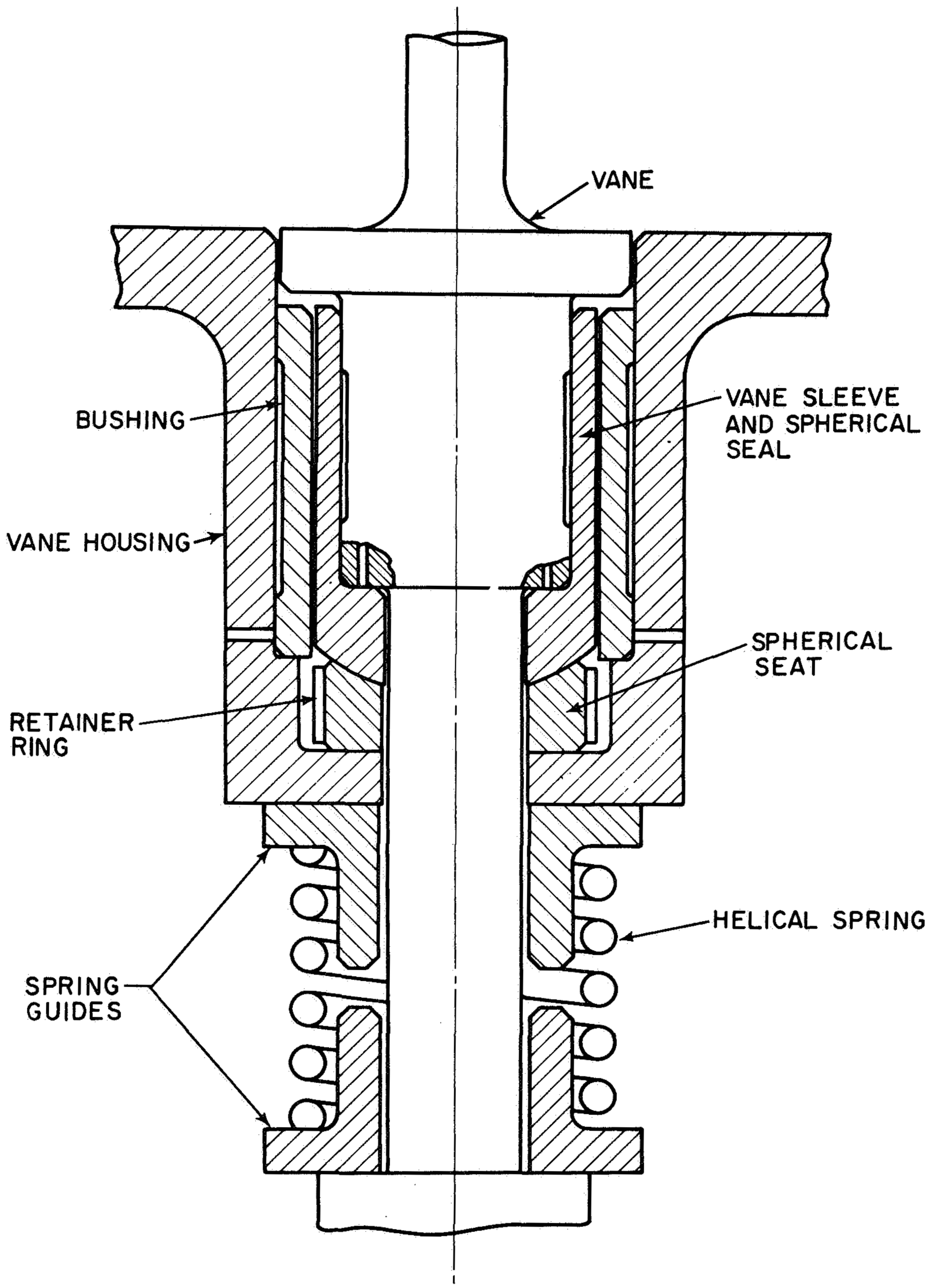

Figure 17 Schematic of Spherical-Seat Vane Pivot Seal

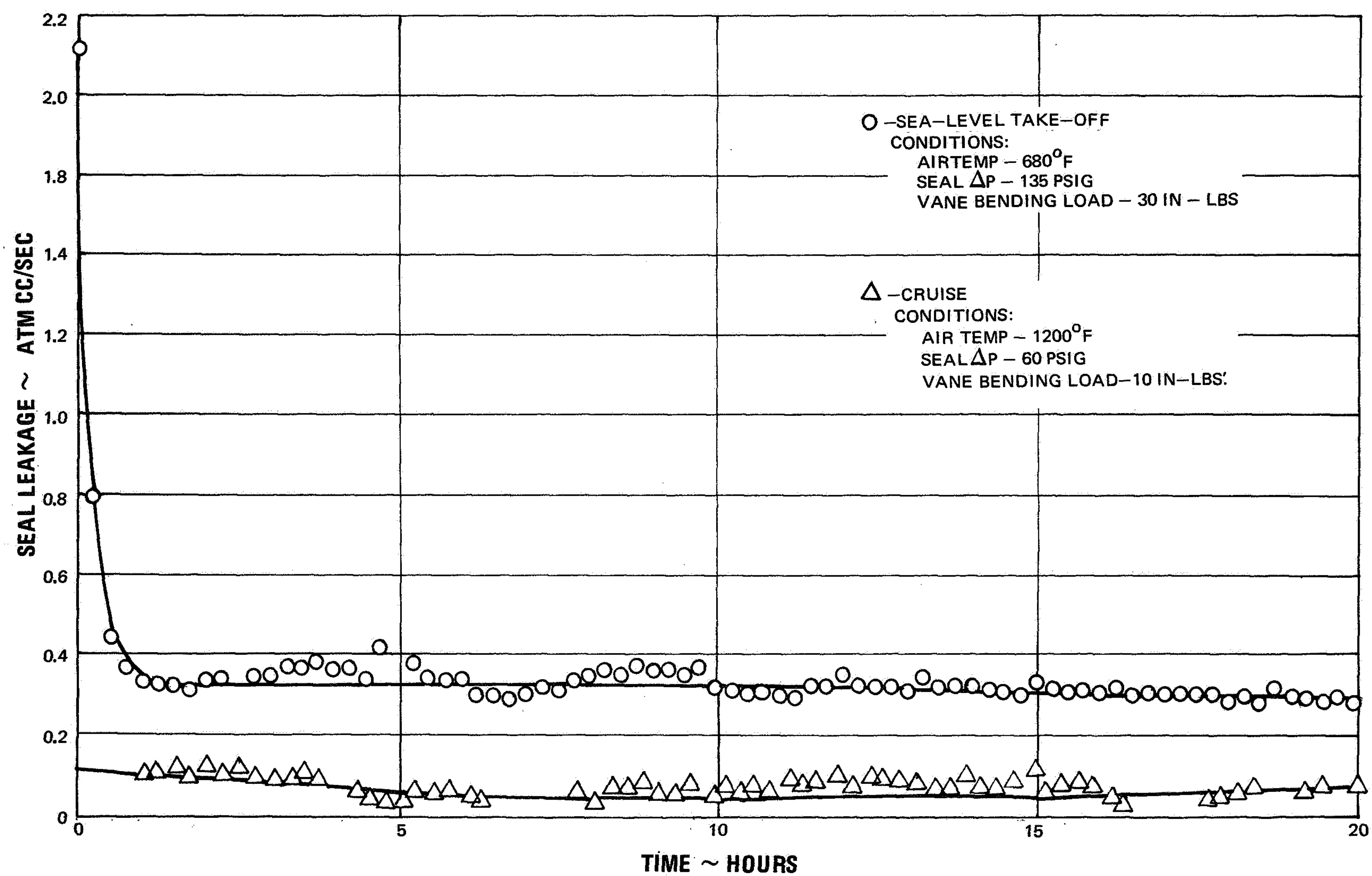

Figure 18 Results of the Endurance Test of the Single-Bellows Vane Pivot Seal

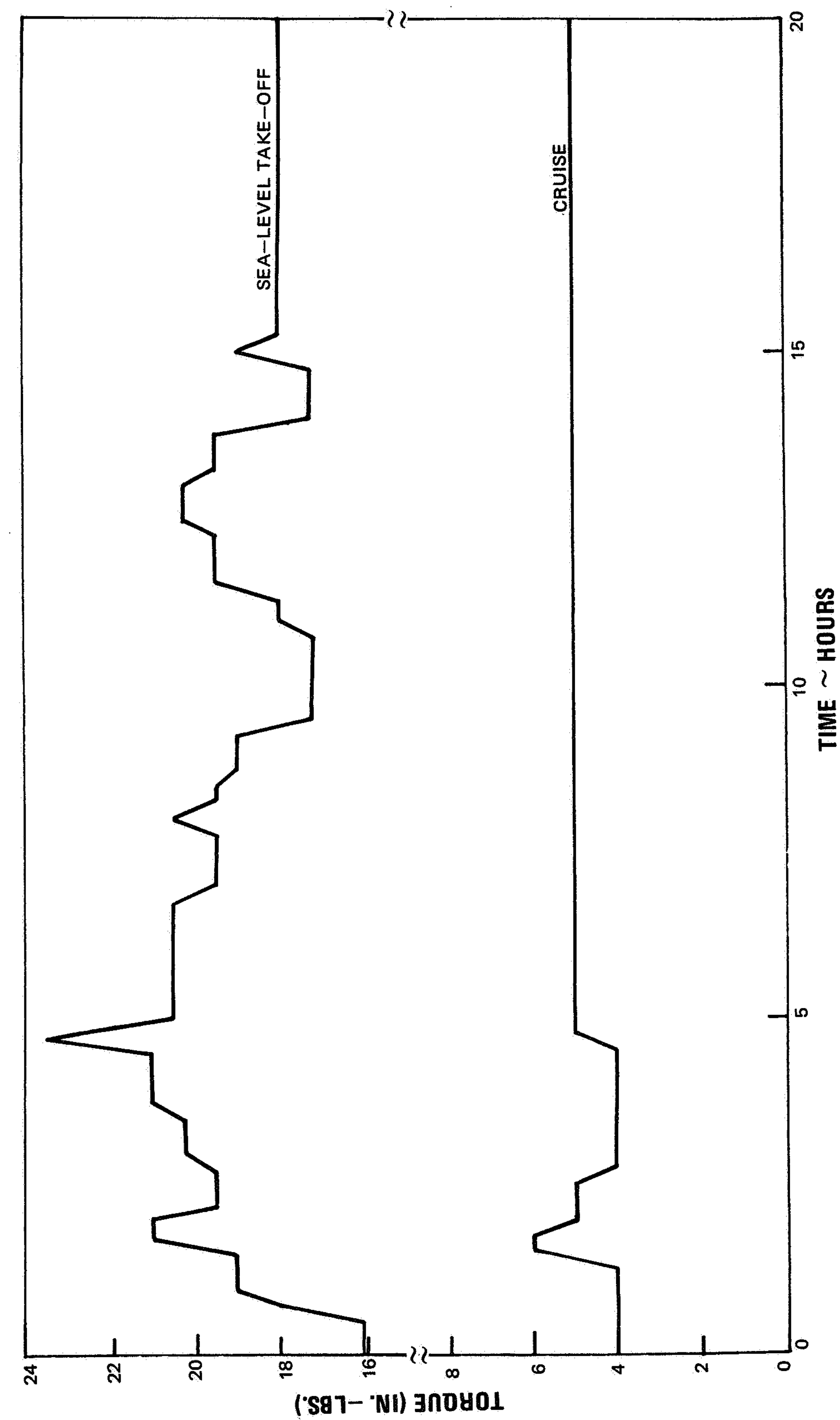

Figure 19 Vane Actuation Torque Required During the Endurance Tests of the Single-Bellows Vane Pivot Seal

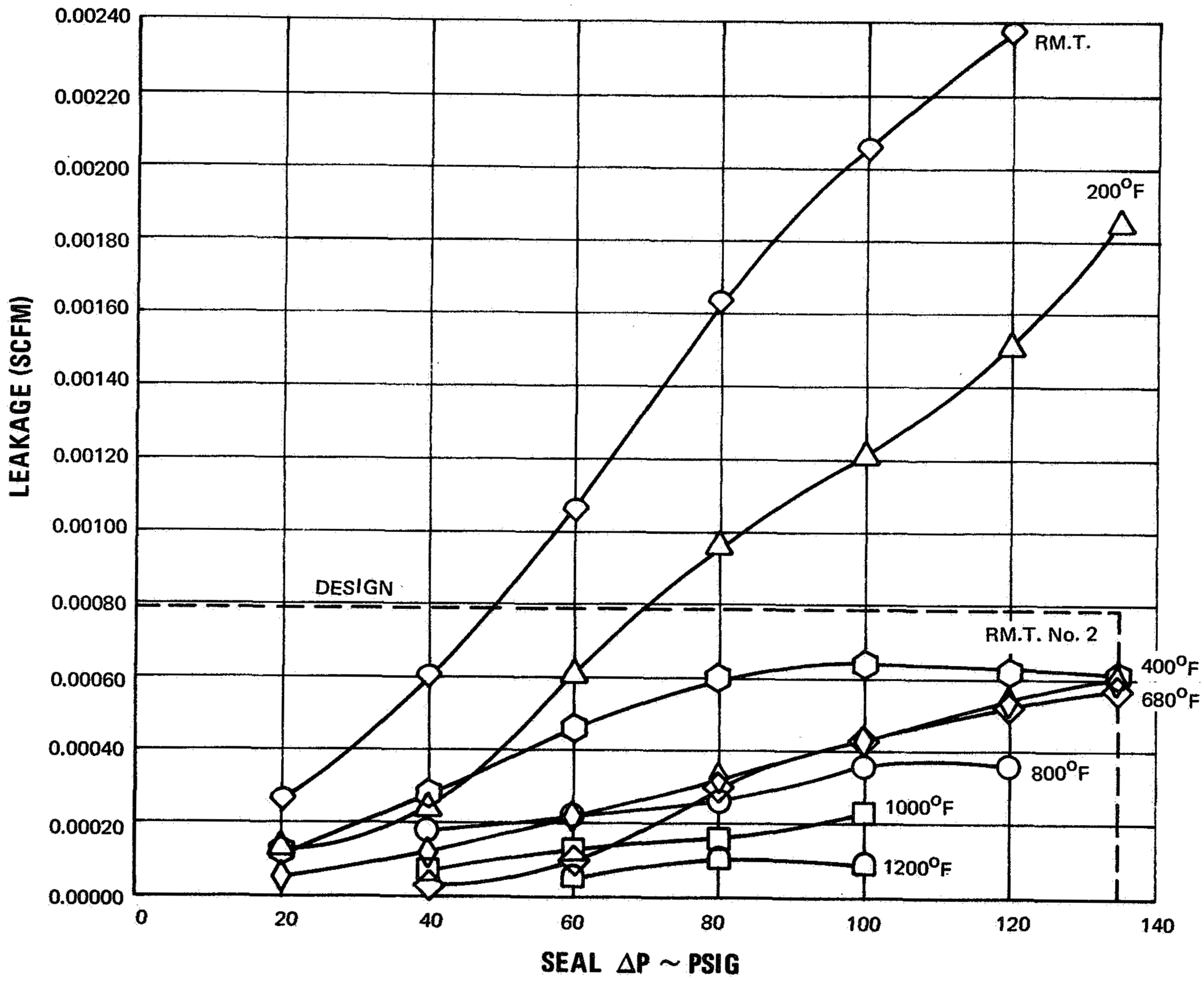

Figure 20 Test Results, Seal Leakage Calibration, Bellows Pivot Seal

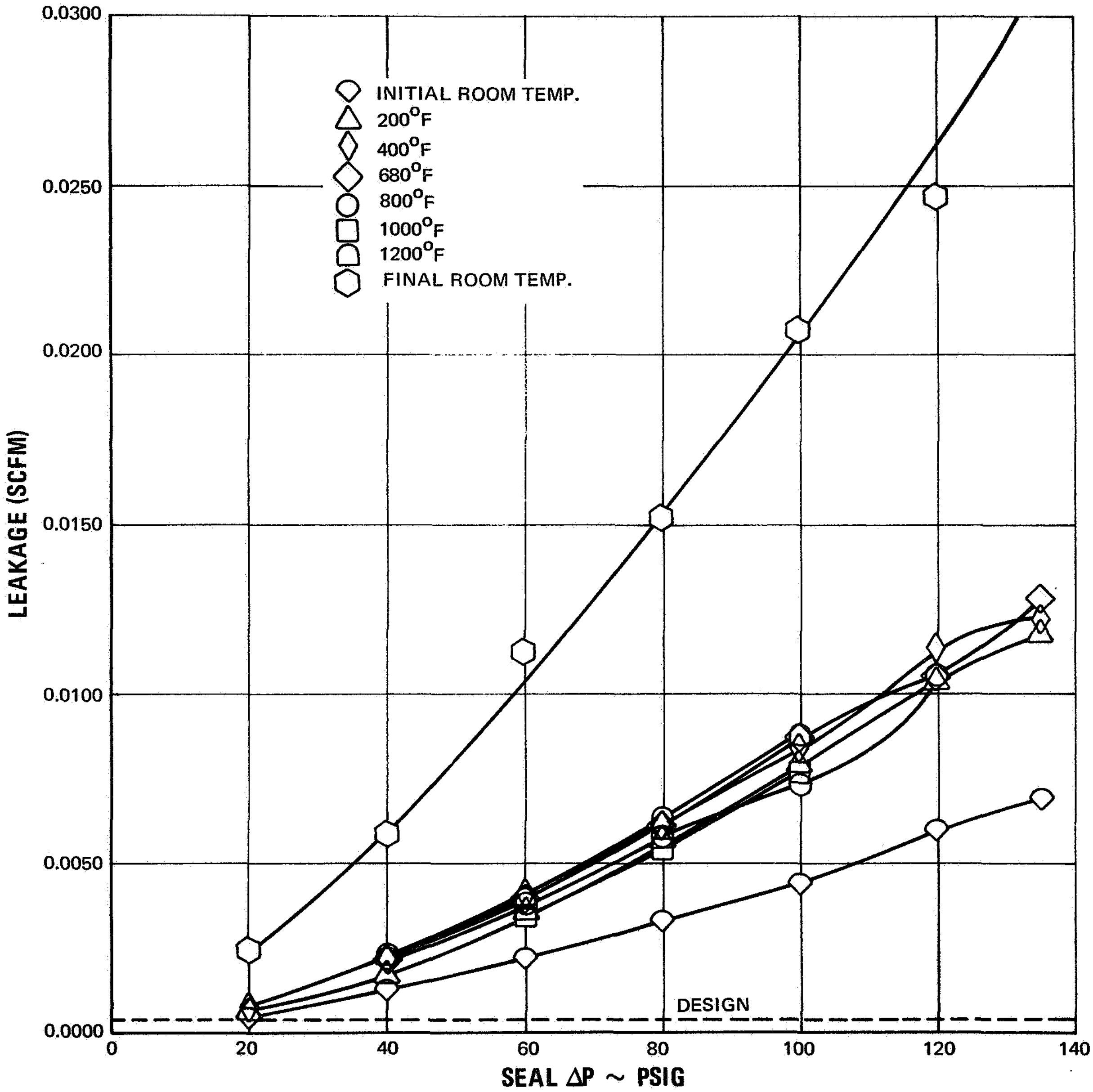

Figure 21 Seal Leakage, Spherical Configuration, Test Unit Number Three

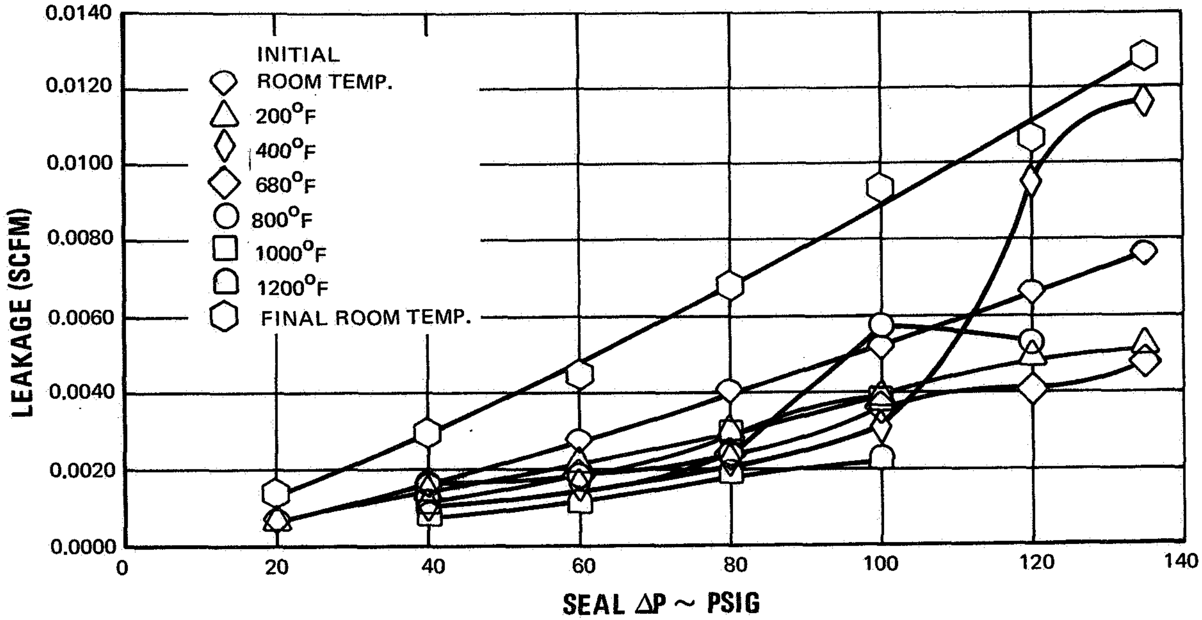

Figure 22 Seal Leakage, Spherical Configuration, Test Unit Number Four

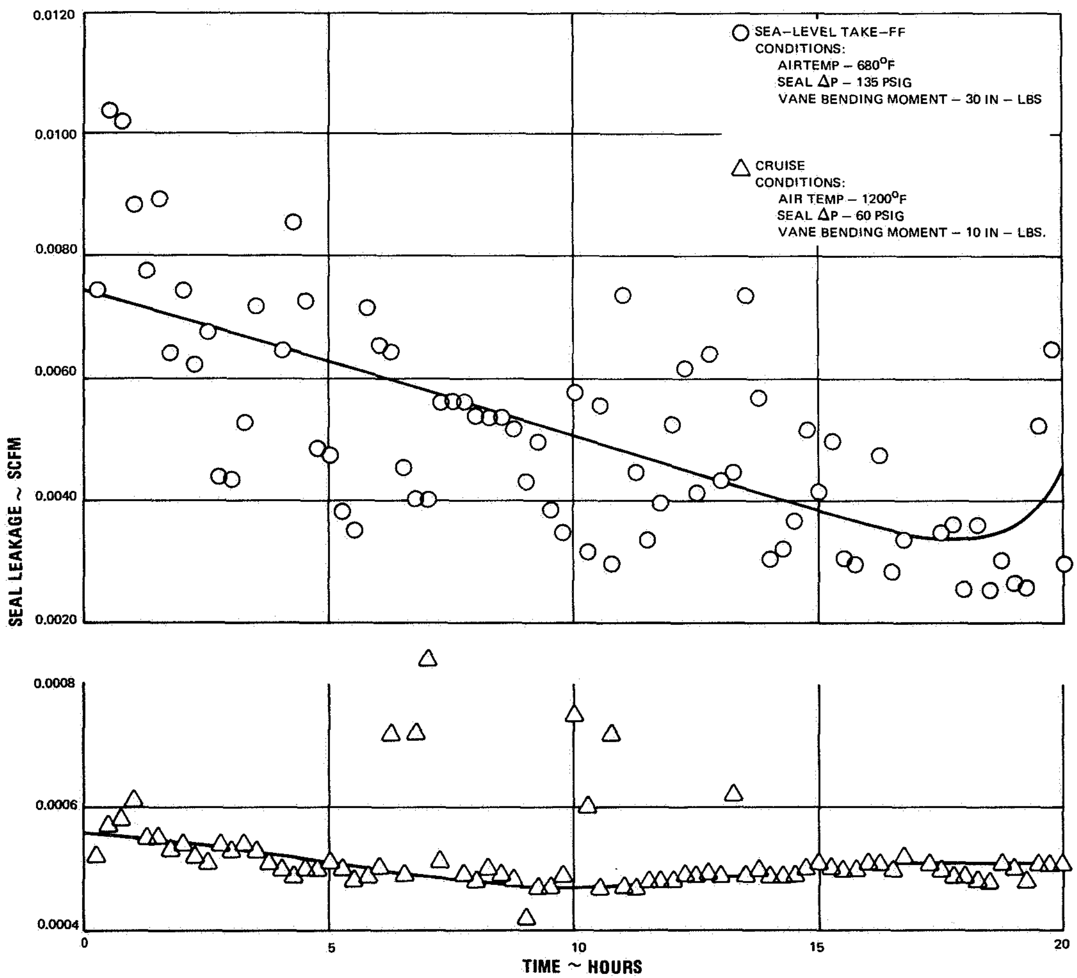

Figure 23 Endurance Results, Test Unit Number Four

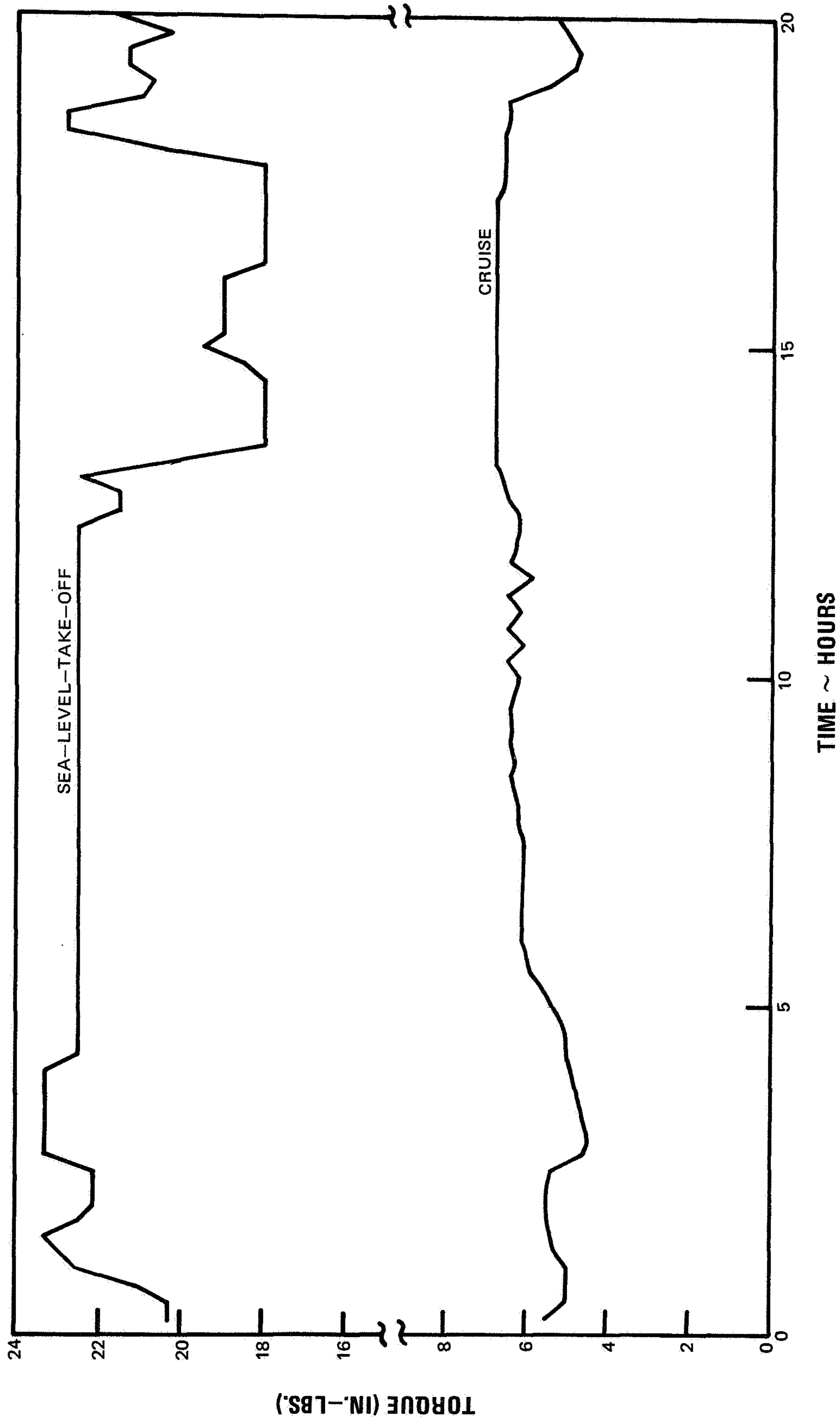

Figure 24 Simulated Vane Actuation Torque, Test Unit Number Four

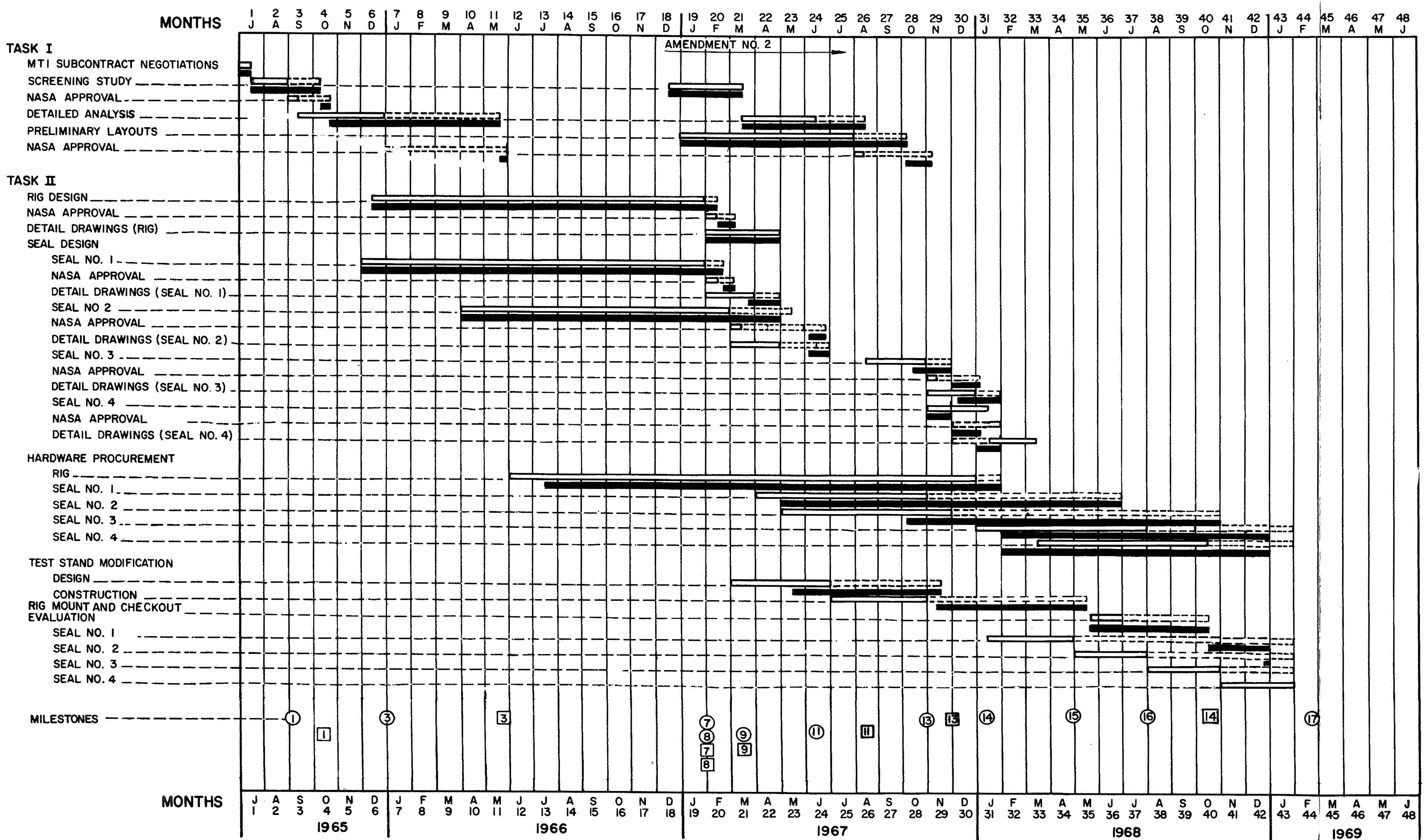

MILESTONES

1. TASK I COMPLETE SCREENING STUDY
2. TASK III COMPLETE SCREENING STUDY
3. TASK I COMPLETE DETAILED ANALYSIS
4. TASK III COMPLETE DETAILED ANALYSIS
5. TASK IV COMPLETE RIG DESIGN
6. TASK IV COMPLETE SEAL DESIGN
7. TASK II COMPLETE RIG DESIGN
8. TASK II COMPLETE SEAL DESIGN (NO. 1)
9. TASK I COMPLETE SCREENING STUDY NO 2
10. TASK IV INITIATE TEST
11. TASK I COMPLETE DETAILED ANALYSIS NO. 2
12. TASK IV COMPLETE EVALUATION OF ONE STATOR PIVOT SEAL
13. TASK II COMPLETE SEAL DESIGN (NO. 3)
14. TASK II INITIATE TEST
15. TASK II COMPLETE EVALUATION OF ONE COMPRESSOR END SEAL
16. TASK II COMPLETE EVALUATION OF ONE STATOR INTERSTAGE SEAL
17. SUBMIT SUMMARY REPORT FOR NASA APPROVAL

LEGEND

WORK PROJECTED
REVISED WORK PROJECTED
WORK ACCOMPLISHED
WORK ACHIEVED EARLY
O ORIGINAL MILESTONE
☐ MILESTONE ATTAINED

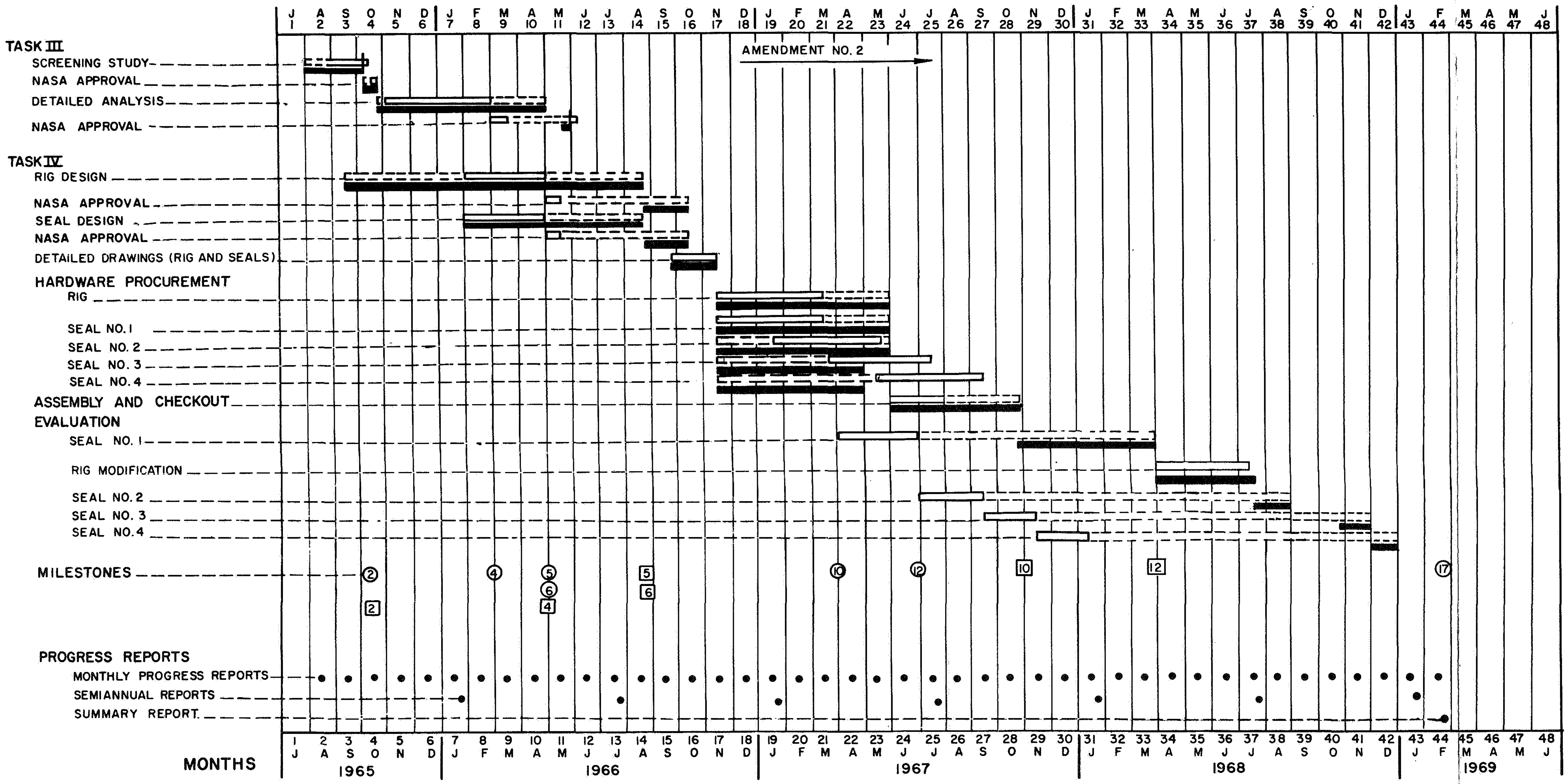

MILESTONES

1. TASK I COMPLETE SCREENING STUDY
2. TASK III COMPLETE SCREENING STUDY
3. TASK I COMPLETE DETAILED ANALYSIS
4. TASK III COMPLETE DETAILED ANALYSIS
5. TASK IV COMPLETE RIG DESIGN
6. TASK IV COMPLETE SEAL DESIGN
7. TASK II COMPLETE RIG DESIGN
8. TASK II COMPLETE SEAL DESIGN (NO.1)
9. TASK I COMPLETE SCREENING STUDY NO. 2
10. TASK IV INITIATE TEST
11. TASK I COMPLETE DETAILED ANALYSIS NO. 2
12. TASK IV COMPLETE EVALUATION OF ONE STATOR PIVOT SEAL
13. TASK II COMPLETE SEAL DESIGN (NO.3)
14. TASK II INITIATE TEST
15. TASK II COMPLETE EVALUATION OF ONE COMPRESSOR END SEAL
16. TASK II COMPLETE EVALUATION OF ONE STATOR INTERSTAGE SEAL
17. SUBMIT SUMMARY REPORT FOR NASA APPROVAL

LEGEND

WORK PROJECTED
REVISED WORK PROJECTED
WORK ACCOMPLISHED
WORK ACHIEVED EARLY
ORIGINAL MILESTONE
MILESTONE ATTAINED

Semiannual Reports Distribution List
NAS 3-7605

Addressee	Number of Copies
1. NASA Headquarters Washington, D.C. 20546	
Attn: N.F. Rekos (RAP)	1
A.J. Evans (RAD)	1
J. Maltz (RRM)	1
2. NASA-Lewis Research Center 21000 Brookpark Road Cleveland, Ohio 44135	
Attn: A. Ginsburg, MS 5-3	1
E.E. Bisson, MS 5-3	1
R.L. Johnson, MS 23-2	1
W.R. Loomis, MS 23-2	1
L.P. Ludwig, MS 23-2	3
M.A. Swikert, MS 23-2	1
D.P. Townsend, MS 6-1	1
C.H. Voit, MS 5-3	1
J.H. DeFord, MS 77-3	1
M.J. Hartman, MS 5-9	1
J.H. Childs, MS 60-4	1
W.H. Roudebush, MS 60-4	1
Report Control Office, MS 5-5	1
Library, MS 60-3	1
Technology Utilization Office, MS 3-19	1
N.T. Musial, MS 501-3	1
3. NASA-Scientific and Technical Information Facility P.O. Box 33 College Park, Maryland 20740 Attn: NASA Representative	6
4. NASA Langley Research Center Langley Station Hampton, Virginia 23365 Attn: Mark R. Nichols	1
5. United States Air Force Wright-Patterson Air Force Base AF Systems Command USAF Wright-Patterson AFB, Ohio 45433	
Attn: AFAPL (APFL), K.L. Berkey and L. DeBrohum	1
AFAPL (APTC), C. Simpson	1
APTP, I.J. Gershon	1
SEJDF, S. Prete	1
MANL, R. Adamczak	1
MANE, R. Headrick	1
MAAE, P. House	1
6. FAA Headquarters 800 Independence Avenue, S.W. Washington, D.C. 20553	
Attn: General J.C. Maxwell	1
F.B. Howard	1
7. U.S. Naval Air Material Center Aeronautical Engine Laboratory Philadelphia, Pennsylvania Attn: A.L. Lockwood	1
8. U.S. Naval Research Laboratory Washington, D.C. Attn. Charles Murphy	1
9. Department of the Navy Bureau of Naval Weapons Washington, D.C.	
Attn: A.D. Nehman, RAAE-3	1
C.C. Singletorry, RAPP-4	1
10. Department of the Navy Bureau of Ships Washington, D.C. Attn: Harry King, Code 634A	1
11. U.S. Navy Marine Engineering Laboratory Friction and Wear Division Annapolis, Maryland Attn: R.B. Snapp	1
12. Commanding Officer U.S. Navy Underwater Weapons Research and Engineering Section Newport, R.I. 02840 Attn: Technical Library T13(A-183)	1
13. Department of the Army U.S. Army Aviation Material Labs. Fort Eustis, Virginia 23604 Attn: John W. White, Chief Propulsion Division	1
14. AVCOM AMSAVEGTT Mart Building 405 South 12th Street St. Louis, Missouri 63100 Attn: E. England	1
15. Aerojet-General Corporation 20545 Center Ridge Road Cleveland, Ohio 44116 Attn: W.L. Snapp	1
16. Avco Corporation Lycoming Division Stratford, Connecticut Attn: R. Cuny	1

Addressee	Number of Copies
17. Battelle Memorial Institute 505 King Avenue Columbus Ohio 43201 Attn: C.M. Allen	1
18. Bendix Corporation Fisher Building Detroit, Michigan 48202 Attn: R.H. Isaacs	1
19. B.F. Goodrich Company Aerospace & Defense-Products Div. Troy, Ohio Attn: L.S. Blalkowski	1
20. Boeing Aircraft Company 224 N. Wilkinson Street Dayton, Ohio 45402 Attn: S.L. Strack	1
21. Borg-Warner Corporation Roy C. Ingersoll Research Center Wolf and Algonquin Roads Des Plaines, Illinois 60018	1
22. Carbon Products Division of Union Carbide Corporation 270 Park Avenue New York, New York 10017 Attn: J. Curran	1
23. Chicago Rawhide Mfg. Co. 1311 Elston Avenue Chicago, Illinois Attn: R. Blair	1
24. Clevite Corporation Cleveland Graphite Bronze Div. 17000 St. Clair Avenue Cleveland, Ohio 44110 Attn: Thomas H. Koenig	1
25. Continential Aviation & Engrg. 12700 Kercheval Detroit, Michigan Attn: A. J. Follman	1
26. Crane Packing Company 6400 Oakton Street Morton Grove, Illinois 60053 Attn: Harry Tankus	1
27. Douglas-McDonnell Corp. Suite 620 333 W. First Street Dayton, Ohio 45402 Attn: R. G. Donmayer	1
28. Durametallic Corporation Kalamazoo, Michigan Attn: H. Hummer	1
29. E.I. duPont deNemours & Co. 1007 Market Street Wilmington, Delaware 19898 Attn: R. B. Lewis Engrg. Service Div.	1
30. Fairchild-Stratos-Western 1800 Rosecrans Ave. Manhatten, Calif. 90266 Attn: Alex D'Angio	1
31. Fairchild-Hiller Corporation Republic Aviation Division Farmingdale, Long Island New York 11735 Attn: C. Collis	1
32. Franklin Institute Laboratories 20th & Parkway Philadelphia, Pennsylvania Attn: J. V. Carlson Otto Decker	1 1
33. Garlock, Inc. Palmyra, New York 14522 Attn: E. W. Fisher	1
34. Garrett Corporation Air Research Mfg. Div. 9851-9951 Sepulvelda Blvd. Los Angeles, Calif. 90009 Attn: A. Silver	1
35. General Dynamics Corporation 5100 W. 164th Street Cleveland, Ohio 44142 Attn: W. Geudtner, Jr.	1
36. General Electric Company Advanced Engine & Technology Dept. Cincinnati, Ohio 45415 Attn: L. B. Venable G. J. Wile C. C. Moore, H-25 W. McCarty	1 1 1 1
37. General Electric Company Electro-Mechanical Eng. Unit Bldg. 55-263 1 River Road Schenectady, New York Attn: E. R. Booser	1

Addressee	Number of Copies
38. General Electric Company Research and Development P.O. Box 8 Schenectady, New York 12301 Attn: G. R. Fox	1
39. General Motors Corporation Allison Division Speedway Indianapolis, Indiana 46206 Attn: E. M. Deckman	1
40. Hughes Aircraft Company Centinela Ave. & Teale St. Culver City, Calif. 90230	1
41. Hyck Metals Company P.O. Box 30 45 Woodmont Road Milford, Connecticut Attn: J. I. Fisher	1
42. I.I.T. Research Foundation 10 West 35th Street Chicago, Illinois 60616 Attn: Dr. Strohmeier	1
43. Industrial Tectonics Box 401 Hicksville, New York 11801 Attn: J. Cherubin	1
44. Koppers Company, Inc. Metal Products Division Piston Ring and Seal Department Baltimore, Maryland Attn: F. C. Kuchler E. Taschenburg	1 1
45. Lockheed Aircraft Company 118 W. First St. Room 1400 Dayton, Ohio 45402 Attn: L. Kelly	1
46. Martin Marietta Corp. Parkview Plaza Office Bldg. 1700 Needmore Road, P.O. Box 14153 Dayton, Ohio 45414 Attn: Z. G. Horvath	1
47. Mechanical Technology, Inc. 968 Albany-Shaker Road Latham, New York Attn: Donald F. Wilcock	1
48. Metal Bellows Corporation 20977 Knapp Street Chatsworth, California Attn: Sal Artino	1
49. Midwest Research Institute 426 Volker Blvd. Kansas City, Missouri Attn: V. Hopkins	1
50. Monsanto Chemical Company 800 North Lindbergh Blvd. St. Louis, Missouri 63106 Attn: K. McHugh R. Hatton	1 1
51. North American Rockwell Corp. 5100 West 164th Street Cleveland, Ohio 44142 Attn: George Bremer	1
52. Northrop Corporation 1730 K Street N.W. Suite 903-5 Washington, D.C. Attn: S. W. Fowler, Jr.	1
53. Pesco Products Division Borg-Warner Corporation 24700 N. Miles Bedford, Ohio	1
54. Pressure Technology Corp. of Am. 453 Amboy Avenue Woodbridge, New Jersey Attn: A. Dobrowsky	1
55. North American Rockwell Corp. Rocketdyne Division 6633 Canoga Avenue Canoga Park, California Attn: M. Butner	1
56. Sealol Inc. P.O. Box 2158 Providence, Rhode Island Attn: Justus Stevens	1
57. SKF Industries, Inc. 1100 First Avenue King of Prussia, Penn. Attn: L. B. Sibley	1
58. Southwest Research Institute 8500 Culebra Road San Antonio, Texas 78206 Attn: P.M. Ku	1
59. Stanford Research Institute Menlo Park, California Attn: R. C. Fey	1